Palaeogeography, Palaeoclimatology, Palaeoecology 373 (2013) 6–24

Contents lists available at SciVerse ScienceDirect

Palaeogeography, Palaeoclimatology, Palaeoecology

journal homepage: www.elsevier.com/locate/palaeo

Improving coral-base paleoclimate reconstructions by replicating 350 years of coral Sr/Ca variations

Kristine L. DeLong [a,b,*], Terrence M. Quinn [c,d], Frederick W. Taylor [c], Chuan-Chou Shen [e], Ke Lin [e]

[a] College of Marine Science, University of South Florida, 140 7th Avenue South, St. Petersburg, FL 33701, USA
[b] Department of Geography and Anthropology, Louisiana State University, 227 Howe-Russell Geoscience Complex, Baton Rouge, LA 70803, USA
[c] Institute for Geophysics, Jackson School of Geosciences, University of Texas at Austin, J.J. Pickle Research Campus, Building 196, 10100 Burnet Road R2200, Austin, TX 78758, USA
[d] Department of Geological Sciences, Jackson School of Geosciences, University of Texas at Austin, 1 University Station C1100, Austin, TX 78712, USA
[e] High-Precision Mass Spectrometry and Environment Change Laboratory (HISPEC), Department of Geosciences, National Taiwan University, No. 1, Sec. 4, Roosevelt Road, Taipei 10617, Taiwan

ARTICLE INFO

Article history:
Received 15 August 2011
Received in revised form 17 August 2012
Accepted 28 August 2012
Available online 10 September 2012

Keywords:
Sr/Ca
Porites
New Caledonia
^{230}Th
Oxygen isotopes

ABSTRACT

Coral-based climate reconstructions are typically based on a single record and this lack of replication leads to questions in regards to chronology accuracy and reliability of the inclusive geochemical variations to record climate viability. Here we present two multi-century coral Sr/Ca records recovered from a *Porites lutea* colony offshore of Amédée Island, New Caledonia (22°28.8′S, 166°27.9′E). The chronology was developed by cross dating the coral Sr/Ca time series and verifying the chronology with high precision absolute ^{230}Th dating. We identify chronological discrepancies of −2.3 and +3.7 years century^{-1} for reconstructions based on a single core with uncertainty increasing after ~250 years. We assess the impact of *Porites* skeletal architecture on coral geochemistry by characterizing centimeter-scale architectural structures with respect to sampling. Optimal sampling paths are those on the slab surface parallel to the growth direction of individual corallites along the central axis of an actively extending corallite fan. Coral Sr/Ca time series extracted from optimal skeletal structures are highly reproducible with a mean absolute difference of 0.021 mmol mol^{-1} or 0.39 °C for monthly determinations. Suboptimal skeletal architecture is characterized by corallites extending through the slab surface, and the coral Sr/Ca determinations derived from suboptimal paths tend to produce a warm bias that varies between +0.04 and +2.30 °C. Disorganized skeletal architecture is characterized by small, terminating, or unclear corallite fans that produce a cold bias of −0.11 to −2.45 °C in coral Sr/Ca determinations. These problematic architecture types also produce biases in coral δ^{18}O determinations, but to a lesser extent. We assess the impact of sampling a coral colony along paths that vary from vertical to horizontal in large and small *Porites* colonies with extension rates >6 mm year^{-1} and we determine there is no significant difference in the coral Sr/Ca records.

1. Introduction

Dendroclimatologists typically extract two cores from a tree, which contain a cross-section of the tree's annual rings, and then they extract cores from many trees within a stand that they cross-date to determine an absolute chronology (Fritts, 1976). Similarly, geologists extract two or more sediment cores per site with staggered core breaks to bridge gaps created by the core barrel length and then they use stratigraphy to align the cores (e.g., Peterson et al., 2000). Even parallel ice cores, such as those from the Greenland Ice Core Project (GRIP) and Greenland Ice Sheet Program (GISP2), provide valuable information that allows glaciologists to refine their chronologies and more importantly verify the climatic variations between these records (Grootes et al., 1993). Replication of proxy records allows paleoclimatologists to improve chronology accuracy and to isolate the climatic signal by averaging the records to reduce non-climatic variability and noise (Fritts, 1976).

Like trees, massive boulder-like corals, such as *Porites* spp., contain annual density bands visible in X-ray images (i.e., X-radiographs) of thin cross sections from the coral skeleton (Knutson et al., 1972; Lough and Cooper, 2011). These coral colonies can grow as high as 7 m (Brown et al., 2009), which allow paleoclimatologists to develop chronologies that span many centuries (Veron, 1986; Corrège, 2006). Coral paleoclimatologists may recover more than a single core from a massive coral colony; however, researchers typically produce a geochemical time series from a single core (e.g., Linsley et al., 1994; Swart et al., 1996a; Quinn et al., 1998; Felis et al., 2000; Kuhnert et al., 2002; Zinke et al., 2004; Calvo et al., 2007) for several reasons including time and budgetary constraints (Dunbar and Cole, 1992; Corrège, 2006).

* Corresponding author at: Department of Geography and Anthropology, Louisiana State University, 227 Howe-Russell Geoscience Complex, Baton Rouge, LA 70803, USA.
E-mail address: kdelong@lsu.edu (K.L. DeLong).

0031-0182/$ – see front matter © 2012 Elsevier B.V. All rights reserved.
http://dx.doi.org/10.1016/j.palaeo.2012.08.019

A single core extracted from a coral colony along the growth axis may be complete with little material missing in core breaks, but this is not typical with larger colonies (e.g., Quinn et al., 1998; Linsley et al., 2000; Urban et al., 2000; Ren et al., 2002). Growth orientation changes on the centimeter scale may produce ambiguous banding patterns in the X-radiographs resulting in locally absent years (Barnes et al., 1989; Lough and Barnes, 1997; Hendy et al., 2003; Alibert and Kinsley, 2008). False bands or stress bands visible in the X-radiographs add to the chronology uncertainty if these bands are counted (Hudson et al., 1976; Swart et al., 1996b). The core extraction process may produce breaks in the core or the core may contain cavities from bioerosion resulting in missing years (Hendy et al., 2003). Therefore, chronology uncertainty on the annual scale increases with age unless independent age verification such as high precision absolute thorium-230 (^{230}Th) dating is used (Shen et al., 2008). Chronology uncertainty is estimated to be ± 1 to 5 years century^{-1} for reconstructions with a single coral core (Swart et al., 1996b; Dunbar and Cole, 1999; Felis et al., 2000; DeLong et al., 2007; Shen et al., 2008).

The inclusive geochemical records in massive corals are assumed to be homogenous within the corallum; however, comparisons between contemporaneous samples reveal some discrepancies (Land et al., 1975; McConnaughey, 1989; de Villiers et al., 1994, 1995; Alibert and McCulloch, 1997; Cohen and Hart, 1997). Synchronous samples extracted from the horizontal and vertical axes of a *Pavona clavus* colony have discrepancies of 2 to 4 °C for coral Sr/Ca and up to 8 °C for coral δ^{18}O and these discrepancies are attributed to differing linear extension rates (McConnaughey, 1989; de Villiers et al., 1994, 1995). The incorporation of the ^{18}O and Sr into the coral skeleton is assumed to have a constant offset from equilibrium with high linear extension rates or growth rates (McConnaughey, 1989; Shen et al., 1996). The reported lower limit for growth-related effects is 6 mm year^{-1} for δ^{18}O determinations in *Porites* spp. (Felis et al., 2003). Concerns with growth-related effects may limit the use of slow growing portions of the corallum or slow growing coral species (Jones et al., 2009). The established sampling method for coral-based reconstructions is to sample a fast growing coral species along the maximum growth axis by recovering a vertical core from the corallum and extracting samples along a vertical path perpendicular to the annual density bands (Fairbanks and Dodge, 1979; Marshall and McCulloch, 2002).

Coral architecture further complicates the extraction of a geochemical signal from the time axis of the corallum. Massive *Porites* spp. have small polyps, along a lenticular or bumpy living surface, calcifying skeletal corallites. These corallites are arranged in three-dimensional fans within the corallum with new corallites forming along the apex of the fan (Veron, 1986; Darke and Barnes, 1993). The fans extend upwards and outwards in three-dimensions until the corallites contact another fan and then the corallite's growth slows, ending with corallites being absorbed in the valley between fans (Barnes and Lough, 1989; Lough and Barnes, 1992; Darke and Barnes, 1993). As the colony expands, new corallite fans form and older fans terminate creating an image of many fans in an X-radiograph (Barnes, 1973; Darke and Barnes, 1993). Comparisons of geochemical determinations between the apex and the valley from the same density band (i.e., same year) reveal that the valleys have higher coral δ^{18}O and Sr/Ca values or 1 °C and 2 °C colder temperatures, respectively (Alibert and McCulloch, 1997; Cohen and Hart, 1997). For massive *Porites* spp., the sampling method has an additional step in which the sampling path follows the apex of a corallite fan and valleys are avoided (Alibert and McCulloch, 1997; Cohen and Hart, 1997; Felis et al., 2000). Other coral species have distinct centimeter-scale architecture that requires different sampling methods for those species (e.g., Leder et al., 1996; Watanabe et al., 2003; Cohen et al., 2004; Smith et al., 2006; Giry et al., 2010).

Following these general sampling methods, researchers have produced temperature reconstructions from the Sr/Ca variations in *Porites* corals that span many centuries (Linsley et al., 2000; Hendy et al., 2002; Linsley et al., 2004; Calvo et al., 2007; DeLong et al., 2012a). Further research identified some discrepancies in coral Sr/Ca reconstructions within records from the same location and/or region calling into question the validity of these reconstructions (Linsley et al., 2006; Calvo et al., 2007). Other researchers found chronological discrepancies when additional coral records were cross-dated within a set of corals from the same location (Hendy et al., 2003; DeLong et al., 2007). These discrepancies clearly outline the need to replicate coral Sr/Ca records in order to isolate the source of these discrepancies and to evaluate the reproducibility and accuracy of this geochemical temperature proxy (Marshall and McCulloch, 2002; Lough, 2004; Jones et al., 2009).

2. Study background

Our replication study with coral Sr/Ca determinations originally made sample extractions from paths parallel to the sampling pathways used to create the New Caledonia coral δ^{18}O record of Quinn et al. (1998) (Fig. 1). Some intervals revealed temperatures inferred from coral Sr/Ca much colder than that inferred from coral δ^{18}O (e.g., 1870 to 1875 Common Era (CE)). Additionally, we found intervals with discrepancies between contemporaneous coral Sr/Ca determinations within the same coral colony as well as nearby coral colonies (DeLong et al., 2007). We decided to investigate the source of these discrepancies by sampling a second core from the same colony to replicate the Sr/Ca determinations. In the process, other discrepancies were detected between the Sr/Ca variations from these two cores.

Here we present the results from our coral Sr/Ca replication study in which we sampled and cross-dated two intracolony cores spanning 350 years. We quantitatively evaluate reproducibility of intracolony geochemical variations, sources of uncertainty, and chronology error. We assess established sampling methods by comparing coral Sr/Ca variations from different skeletal structures and sampling path orientation with respect to the colony (i.e., horizontal and vertical axes). We further tested these sampling methods with a small colony from Vanuatu. We verify our chronology and cross dating methods with absolute ^{230}Th dating. We make recommendations for improving coral-based paleoclimate reconstructions based on our experiences. A separate paper assesses the number of coral colonies needed to isolate the temperature signal on various time scales as well as the sources of non-temperature variability including subannual chronology uncertainties (DeLong et al., in revision). We discuss the climatic interpretation of the 350 year-long temperature reconstruction in a separate paper (DeLong et al., 2012a).

3. Methods

3.1. Coral sampling

This study examines cores extracted from a large (~4 m) live *Porites lutea* colony (PAA) located adjacent to Amédée Island, New Caledonia (22°28.8′S, 166°27.9′E) with details of the study site and cores previously described (Quinn et al., 1996, 1998; Stephans et al., 2004; DeLong et al., 2007). The cores sampled by this study are from the same massive coral colony and include: two long cores, 92-PAA1 and 92-PAA2, recovered in July 1992 CE; and a smaller core, 99-PAA, recovered in December 1999 CE (Figs. 1 and 2). The cores were recovered from the vertical axis of the colony with breaks between core sections. Additionally, we collected in 1979 CE a small *P. lutea* colony, 270 mm wide and 170 mm high, offshore of Tasmaloum, Republic of Vanuatu (15° 37.512′S, 167°13.947′E). This colony was sampled following the same methods as the Amédée Island cores with paths oriented at 0°, 25°, 85°, and 90° from vertical. The results from this Vanuatu coral are previously mentioned as unpublished results (DeLong et al., 2010) and one path from this coral is presented previously (Ourbak et al., 2008).

The cores were cut longitudinally, along the axis of growth, to reveal medial transects of the corallites and corallite fans and 5 mm slabs were extracted from one core half. The slabs were cleaned

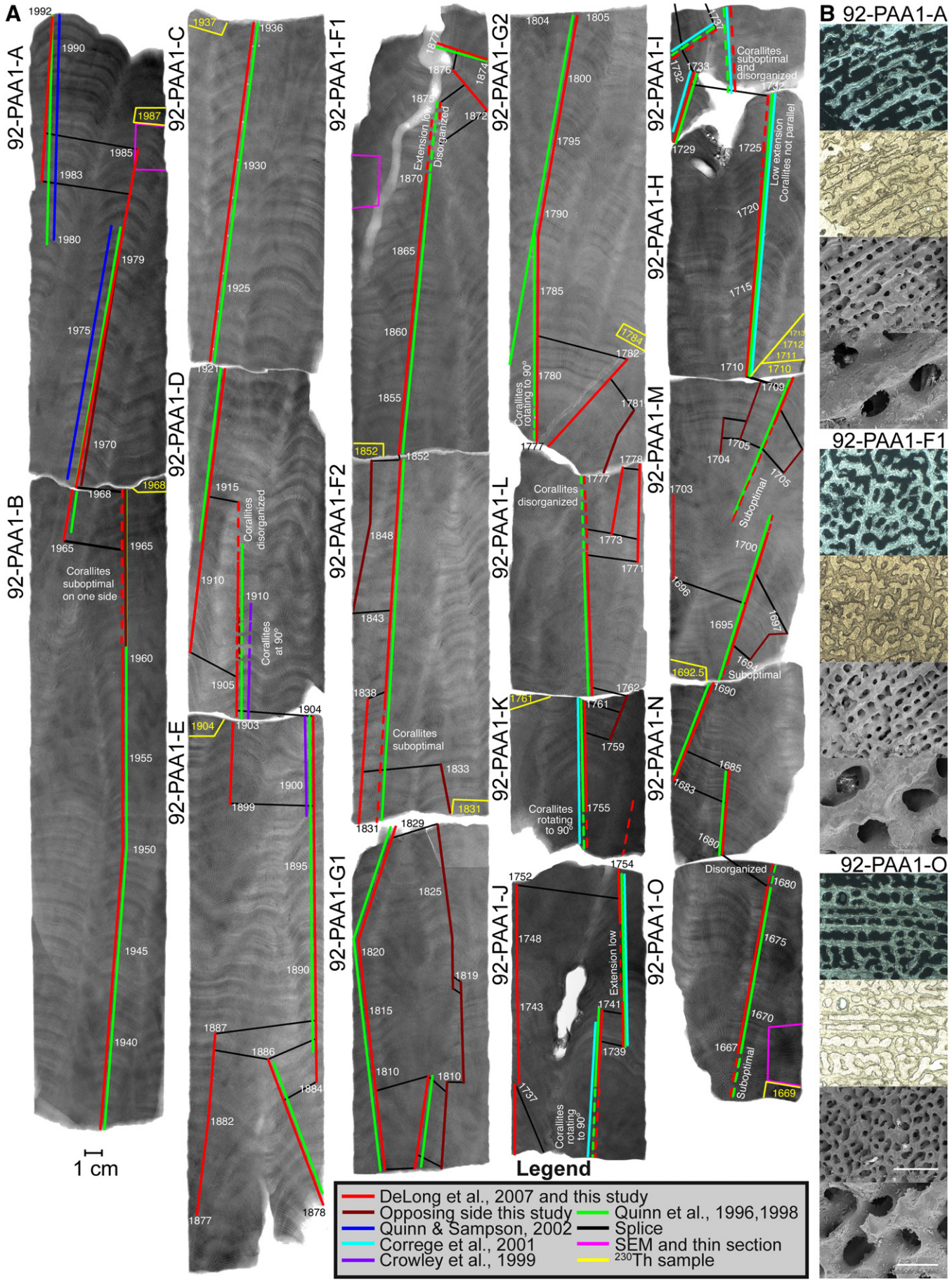
A
92-PAA1-A
92-PAA1-B
92-PAA1-C
92-PAA1-D
92-PAA1-E
92-PAA1-F1
92-PAA1-F2
92-PAA1-G1
92-PAA1-G2
92-PAA1-H
92-PAA1-I
92-PAA1-J
92-PAA1-K
92-PAA1-L
92-PAA1-M
92-PAA1-N
92-PAA1-O
Corallites suboptimal on one side
Corallites disorganized
Corallites at 90°
Extension low
Disorganized
Corallites rotating to 90°
Corallites suboptimal
Corallites suboptimal and disorganized
Low extension
Corallites not parallel
Suboptimal
Extension low
Corallites rotating to 90°
Disorganized
Suboptimal
1 cm
B 92-PAA1-A
92-PAA1-F1
92-PAA1-O
Legend
DeLong et al., 2007 and this study
Opposing side this study
Quinn & Sampson, 2002
Correge et al., 2001
Crowley et al., 1999
Quinn et al., 1996,1998
Splice
SEM and thin section
230Th sample

with an ultrasonicator in deionized water and allowed to air-dry. The slabs were X-rayed (Quinn et al., 1996, 1998) and then scanned at 4720 pixels mm^{-1} with a Microtek© 1000XL scanner to create digital images that were compiled into a multi-layer digital image (Figs. 1 and 2). Linear extension was determined by measuring the distance between high-density bands in the X-radiographs and by the difference in depth (i.e., mm from the first sample for each path) between winter maxima (August) in coral Sr/Ca. Extension per year was monitored for possible growth-related effects and problematic sampling (see Section 5.1). Samples were extracted from the top, middle, and bottom of 92-PAA1 and from the bottom of 92-PAA2-M for thin section and scanning electron microscope (SEM) analysis to check for diagenesis (Figs. 1 and 2), which is standard protocol for coral reconstructions (Quinn and Taylor, 2006).

Samples for geochemical analysis were extracted from the surface of the coral slabs in a continuous path using a computer-driven micromill system (Quinn et al., 1996) with a 1.4 mm diameter dental drill bit and a sampling depth of ~1 mm (DeLong et al., 2007). Sampling intervals were approximately monthly for the Amédée Island samples (Table 1) and approximately monthly and fortnightly (0.83, 1.67 mm $sample^{-1}$, respectively) for the Vanuatu samples. Details of sample path selection are given in Section 4.1.1.

3.2. Geochemical analysis

Elemental ratio and stable isotopic determinations were made from splits of the homogenized coral sample using instrumentation at the University of South Florida (USF) and the University of Texas (UT) following the analytical method previously described (DeLong et al., 2007). Sr/Ca precision determined by the analysis of an internal gravimetric standard (IGS) was ± 0.010 mmol mol^{-1} (1σ; $n=2445$) and by an additional coral standard of a homogenized powder from a *Porites lutea* (PL) was ± 0.018 mmol mol^{-1} (1σ; $n=3343$). Stable isotope precision for $\delta^{18}O$ and $\delta^{13}C$ determined by analysis of NBS19 was ± 0.06‰ and ± 0.04‰ (1σ; $n=324$) for $\delta^{18}O$ and $\delta^{13}C$, respectively. Isotopic ratios are reported in delta (δ) notation relative to Vienna Pee Dee Belemnite (VPDB).

3.3. Establishing chronology

The annual and monthly chronologies were developed using the chronology method described by DeLong et al. (2007) with some modifications due to record length. Temperature records used for the depth to time conversion include in situ sea surface temperature (SST) from Amédée Island (IRD SST) for the interval from 1967 to 1999 CE, regional SST (HadISST_AI) from the 1° grid box centered on our study site from the HadISSTv1.1 data set (Rayner et al., 2003) for the interval from 1870 to 1967 CE, and a time series composed of repeating monthly averages, determined from IRD SST, for the interval from 1649 to 1869 CE. Coral Sr/Ca maxima (minima) were aligned to SST minima (maxima) for each annual cycle with additional tie points for mid-spring and mid-autumn to maximize alignment between records (Paillard et al., 1996; DeLong et al., 2007). The cores were cross-dated by maximizing correlation and verifying with X-radiographs making adjustments for core breaks and discontinuities. Additional paths were sampled to complete the record (Figs. 1 and 2). A master chronology was generated after 1) assessing the cores for missing years caused by breaks in the cores, 2) noting locally absent years resulting from sample path selection, and 3) checking local mean Sr/Ca values on ~20 year intervals for differences between paths resulting from sample path selection (Section 4.1.2).

The coral chronology was verified with high-precision ^{230}Th dating (Shen et al., 2008) carried out at the High-Precision Mass Spectrometry and Environment Change Laboratory (HISPEC) in the Department of Geosciences of the National Taiwan University. Eleven samples for ^{230}Th dating were extracted from a single year from the core 92-PAA1 at intervals ranging from 19 to 49 years (Fig. 1). Uranium–thorium chemistry (Shen et al., 2003) was performed on 13 July 2005 with instrumental analysis on a Thermo Element inductively coupled plasma sector field mass spectrometer (ICP-SF-MS) (Shen et al., 2002). For additional samples from core section 92-PAA1-H, chemistry (Shen et al., 2003) was performed on 18 November 2008 with instrumental analysis on a Thermo Fisher Neptune multicollector inductively coupled plasma mass spectrometer (MC-ICP-MS) (Frohlich et al., 2009; Shen et al., 2010).

3.4. Data analysis

The transfer function of 0.054 mmol mol^{-1} $°C^{-1}$ was determined for these coral cores (DeLong et al., 2007) and was used to convert coral Sr/Ca values to SST. Monthly anomalies were determined with respect to the calibration interval from 1967 to 1999 CE. Significance was assessed using degrees of freedom (*df*) determined with the runs test (Draper and Smith, 1998). Other data analysis methods are described in DeLong et al. (2007).

4. Results

This study extends the interval of the previous study (1900–1999 CE; DeLong et al., 2007) to 1649 CE. Examination of X-radiographs, SEM images, and thin section photomicrographs reveals no evidence of secondary minerals (Figs. 1 and 2). Annual linear extension rates average ~10 mm $year^{-1}$ for 92-PAA1 and 92-PAA2 (Table 1). We identified 15 years with low extension rates (<6 mm $year^{-1}$). The coral Sr/Ca determinations for these low extension years are within analytical precision with synchronous determinations from the other core, which had higher extension rates, except for one year in 92-PAA1 (1817 CE; $\Delta=0.027$ mmol mol^{-1} between annual averages) and two years in 92-PAA2 (1695 and 1697 CE; $\Delta=0.057$ and 0.037 mmol mol^{-1} between annual averages, respectively). There are two years (1701 and 1702 CE) in 92-PAA1 for which no replicate samples are available; these years have the lowest annual extension rate (4.9 mm $year^{-1}$). Correlation between optimally sampled annual average Sr/Ca and annual extension rate is −0.24 for 92-PAA1 ($n=303$, $df=233$, $p<0.001$) and −0.01 for 92-PAA2 ($n=324$, $df=154$, $p=0.78$). Results from core 99-PAA are discussed in previous studies (Stephans et al., 2004; DeLong et al., 2007) and are included in the figures for completeness.

4.1. Reproducibility of coral Sr/Ca

Coral Sr/Ca time series from 92-PAA1 and 92-PAA2 are compared on various timescales (Figs. 3, 4, and Table 1). The means, standard deviations, and range of annual cycles are not significantly different ($p=$ 0.69, 0.29, 0.10, respectively). The Pearson correlation coefficient between the monthly coral Sr/Ca time series is 0.94 ($n=3582$, $df=975$, $p<0.001$), 0.51 for monthly anomalies ($n=3582$, $df=1026$, $p<0.001$), and 0.65 for annual averages ($n=290$, $df=207$, $p<0.001$). The

Fig. 1. Coral X-radiographs of 92-PAA1. (a) Positive X-radiographs of coral slabs in which darker areas are denser and vice versa. Core section names appear to the left side of the section. Years determined by this study are labeled in white. Paths sampled for this study and previous studies indicated by solid color lines (Quinn et al., 1996, 1998; Crowley et al., 1999; Corrège et al., 2001; Quinn and Sampson, 2002; Stephans et al., 2004; DeLong et al., 2007), with black lines indicating a splice between contemporaneous paths (see Legend). White text denotes areas with suboptimal corallite alignment or problematic intervals for discerning chronology. Broken lines are discarded core sections with problematic paths. (b) Thin section photomicrographs viewed under (top) cross-polarized light plane and (bottom) transmitted light (field of view = 2.6 mm). SEM images with scale bars representing 1 mm (top) and 0.2 mm (bottom). Location of thin section, SEM, and ^{230}Th samples are labeled in the X-radiographs; see Legend.

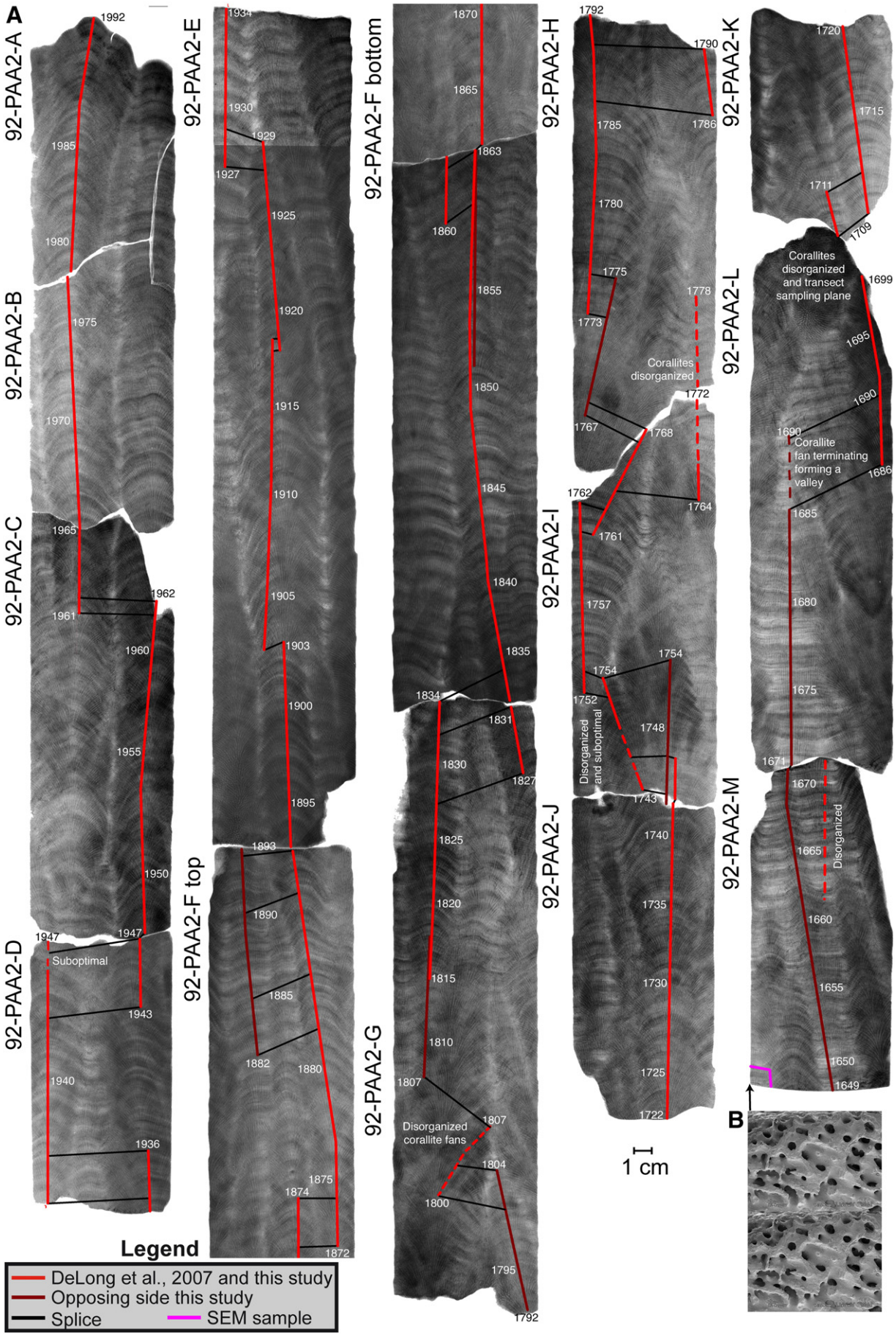
A
92-PAA2-A
92-PAA2-B
92-PAA2-C
92-PAA2-D
92-PAA2-E
92-PAA2-F top
92-PAA2-F bottom
92-PAA2-G
92-PAA2-H
92-PAA2-I
92-PAA2-J
92-PAA2-K
92-PAA2-L
92-PAA2-M
Suboptimal
Corallites disorganized
Disorganized and suboptimal
Disorganized corallite fans
Corallites disorganized and transect sampling plane
Corallite fan terminating forming a valley
Disorganized
B
1 cm
Legend
DeLong et al., 2007 and this study
Opposing side this study
Splice
SEM sample

Table 1
Summary of monthly coral Sr/Ca variations.[a]

Statistic	92-PAA1	92-PAA2	PAA [b]
Mean	9.200	9.201	9.199
Median	9.202	9.201	9.200
Standard deviation	0.103	0.101	0.101
Maximum	9.442	9.464	9.453
Minimum	8.930	8.900	8.911
n [c]	3764	3943	4211
Extension [d]	10.1 ± 2.2	9.9 ± 2.2	
Years [e]	1667–1992	1649–1992	1649–1999
Sampling [f]	0.70	0.83	

[a] Determined in time domain. Units are mmol mol^{-1} unless otherwise indicated.
[b] PAA is the average of 92-PAA1, 92-PAA2 (this study), and 99-PAA (Stephans et al., 2004; DeLong et al., 2007).
[c] Number of observations (n).
[d] Determine between winter maxima (August) in Sr/Ca for each year. Units are mm year^{-1} and reported as an average ± 1 standard deviation.
[e] Each series spans a different time interval; dates are CE.
[f] Sampling interval (mm sample^{-1}).

intracolony time series are coherent in the frequency domain in the interannual to centennial periodicities for the interval from 1728 to 1992 CE, an interval for which both cores are continuous.

We examine the differences between the two monthly coral Sr/Ca time series using two different metrics to assess reproducibility. The absolute difference (AD) is a measure of the discrepancy between two coral Sr/Ca determinations for any single month (Eq. (1)) for which the true coral Sr/Ca value is unknown.

$$AD = 2^{-1/2} |\, \mathrm{coralSr/Ca}_{92-PAA1} - \mathrm{coralSr/Ca}_{92-PAA2} \,| \quad (1)$$

The average of the AD for monthly coral Sr/Ca variations (0.021 ± 0.016 mmol mol^{-1}, 1σ; equivalent to 0.39 °C) is less than 2σ of the magnitude of analytical precision (0.040 mmol mol^{-1} for IGS), which is within the AD reported previously (DeLong et al., 2007). For monthly anomalies, the average AD increases (0.031 ± 0.024 mmol mol^{-1}, 1σ; equivalent to 0.57 °C); however, this includes subannual dating uncertainties of ±3 months resulting from the assignment of any one coral Sr/Ca determination to a particular month. If we smooth the monthly anomalies with a 7-month low pass finite impulse response (LPFIR) filter (Bloomfield, 2000), the AD is reduced (0.025 ± 0.019 mmol mol^{-1}, 1σ; equivalent to 0.46 °C). For most paleoclimate reconstructions, the timescales of interest are greater than annual; therefore, we smoothed the monthly anomalies with a 24-month LPFIR filter and the AD is less than 1σ of the magnitude of analytical precision (0.013 ± 0.009 mmol mol^{-1}, 1σ; equivalent to 0.24 °C; Fig. 4). Monthly variations from cores 92-PAA1 and 92-PAA2 are within 2σ of analytical precision for most of the record except for a few intervals, 1680 to 1685 CE and 1694 to 1696 CE (Fig. 4), in which the number of sampling paths is reduced and gaps occur between the cores.

Another assessment of the reproducibility is the root mean squared (RMS) deviation between coral Sr/Ca determinations for any single month (Sr/Ca_i) and the mean of those determinations (Sr/Ca_{mean}; Eq. (2)), which assumes the mean is a good estimate of the true Sr/Ca value, normalized by the number of observations (n).

$$RMS = \left(\sum (Sr/Ca_i - Sr/Ca_{mean})^2 / n \right)^{1/2} \quad (2)$$

Average RMS for monthly coral Sr/Ca variations (0.015 ± 0.011 mmol mol^{-1}, 1σ; equivalent to 0.28 °C) is within 1σ of our analytical precision (± 0.010 and ± 0.018 mmol mol^{-1}, for IGS and PL, respectively). We find no evidence for a shift in AD or RMS related to the depth to time conversion in regards to the time intervals in which we switch from SST records to climatological averages. The AD and RMS cannot be assessed for periods with only one record; therefore, these determinations should not be considered error free.

4.1.1. Optimal orientation

We have determined that the optimal orientation for a sampling path is along the central axis of a medial transect (i.e., along the middle of the radius) of a corallite fan with individual corallites extending parallel to the slab surface (Fig. 5). Corallite fans are ~20 to 50 mm across and up to 470 mm long and resemble a feather on the slab surface if the slab transects the fan along the growth axis (Fig. 5). Under magnification, medial transects of the corallites reveal long vertical septa or "rods" extending for several centimeters and smaller horizontal synapticulae or "rungs" between septa, ~0.1 mm long (Fig. 5b). These corallite structures resemble ladders when the corallites extend parallel to the slab surface (Fig. 5b) resulting in X-radiographs with clear and distinct density bands (Darke and Barnes, 1993). The optimal sampling path follows the central axis of the "feather" or corallite fan visible on the slab surface in which the "ladders" or septa and synapticulae are parallel to the surface; this optimal path is along the growth or time axis of the corallum (Fig. 5a).

We find the coral Sr/Ca determinations from optimally sampled paths are within analytical precision on monthly to centennial time scales (Figs. 3 and 4). The interval from 1702 to 1705 CE in 92-PAA1-M has higher coral Sr/Ca values (i.e., colder temperatures) and lower extension rates (4.9 to 7.0 mm year^{-1}; Figs. 1, 3, and 4). These corallites are parallel to the slab surface; however, the corallite fan structure is difficult to discern in the X-radiograph (Fig. 1). Unfortunately, there are no coeval paths available for comparison; therefore, we assume these colder temperatures are real. We compare sampling paths slightly off the central axis of the corallite fan with a path along the apex of an adjoining fan in which both paths had corallites parallel to the surface (Fig. 5c). We find approximately the same coral Sr/Ca values for both paths, although winter values tend not to capture the same degree of cooling (Fig. 5d) yet this is not the case for all paths off the central axis (Fig. 6d).

4.1.2. Problematic sampling paths

Two types of coral skeletal architecture present problems in terms of producing robust geochemical records (Figs. 6, 7 and Table 2). The first type of problematic sampling path has corallites extending at angle in the depth (z) dimension relative to the slab surface (x–y plane in Fig. 6a) with the tops of the corallites and their radial structure visible on the slab surface as an oblong transverse cross section. We refer to this type of problematic sampling as "suboptimal" because the angle of the corallites with respect to the slab surface is not parallel or "optimal" but at some angle up to 90° from parallel. Suboptimal skeletal regions can appear as long years in X-radiographs (>15 mm for our coral) resulting in more samples per year, which tend to be lower coral Sr/Ca values (i.e., warmer) relative to contemporaneous samples with optimal orientation. These suboptimal paths result in mean shifts of +0.04 to +2.30 °C depending on the angle of the corallites to the surface with larger shifts associated with perpendicular corallites (Table 2). Suboptimal intervals may span 1 to 9 years in these coral slabs (Table 2).

Suboptimal corallite alignment is readily observed in core section 92-PAA1-K (Fig. 6d and Table 3). The corallites in the top 29 mm of this core section are parallel to the slab surface (optimal orientation) with clear density bands visible in the X-radiograph and extension rates are normal (8.7 mm year^{-1}, $n = 2$). The coral Sr/Ca and $\delta^{18}O$ determinations from this interval have the expected annual cycle (range and number of samples) and the coral Sr/Ca variations agree with contemporaneous samples from 92-PAA2. In the middle of this core section (29.1 to 60.5 mm), the corallites are rotating in

Fig. 2. Coral X-radiographs of 92-PAA2. (a) Positive X-radiographs same as Fig. 1. Paths sampled in this study and a previous study (DeLong et al., 2007) indicated by solid lines, see Legend. (b) SEM images with scale bars representing 0.5 mm (top) and 0.25 mm (bottom).

the depth direction (z) and are oblong relative to the slab surface creating a scallop-edge texture on the surface (Fig. 6b). The density band couplets are elongated in the X-radiographs without sharp boundaries (Fig. 6d) and the distance between these high-density bands is widening (13.3 mm year^{-1}, $n=2$) with the number of samples per year increasing, when a constant sampling interval is used. These additional samples tend to occur in the warmer months thus producing more samples with lower than average coral Sr/Ca and δ^{18}O values (i.e., warmer SST). At the bottom of this core section (60.6 to 92.0 mm), small round circles are visible in the X-radiograph, the density bands disappear, and the apparent extension is longer than expected (40.6 mm year^{-1}, $n=1$). Examination of the slab surface reveals the corallites are at 90° with respect to the slab surface and the circular radial structure of the corallites is visible (Fig. 6c). These perpendicular corallites have increase in the number of lower than average coral Sr/Ca and δ^{18}O values (i.e., warmer SST) and no annual cycle is present in the geochemistry. The earlier study (DeLong et al., 2007) concluded coral δ^{18}O determinations are not influenced by suboptimal corallite orientation for the interval they examined (1960 to 1965 CE; 92-PAA1-B); however, examination of 92-PAA1-K and other core sections reveals that this may not be true for all suboptimal intervals (Figs. 6d, 7, Tables 2 and 3).

The second type of problematic sampling path, called "disorganized," has no visible robust extending corallite fan in the X-radiograph or slab surface. Disorganized corallite fans include merging or terminating fans, fans with low density, small or new fans, and fans with low extension rates related to cavities in the colony. Samples derived from core sections with disorganized corallites tend to have higher coral Sr/Ca values (i.e., colder, –0.11 to −2.45 °C on average; Table 2) and may have reduced apparent extension rates

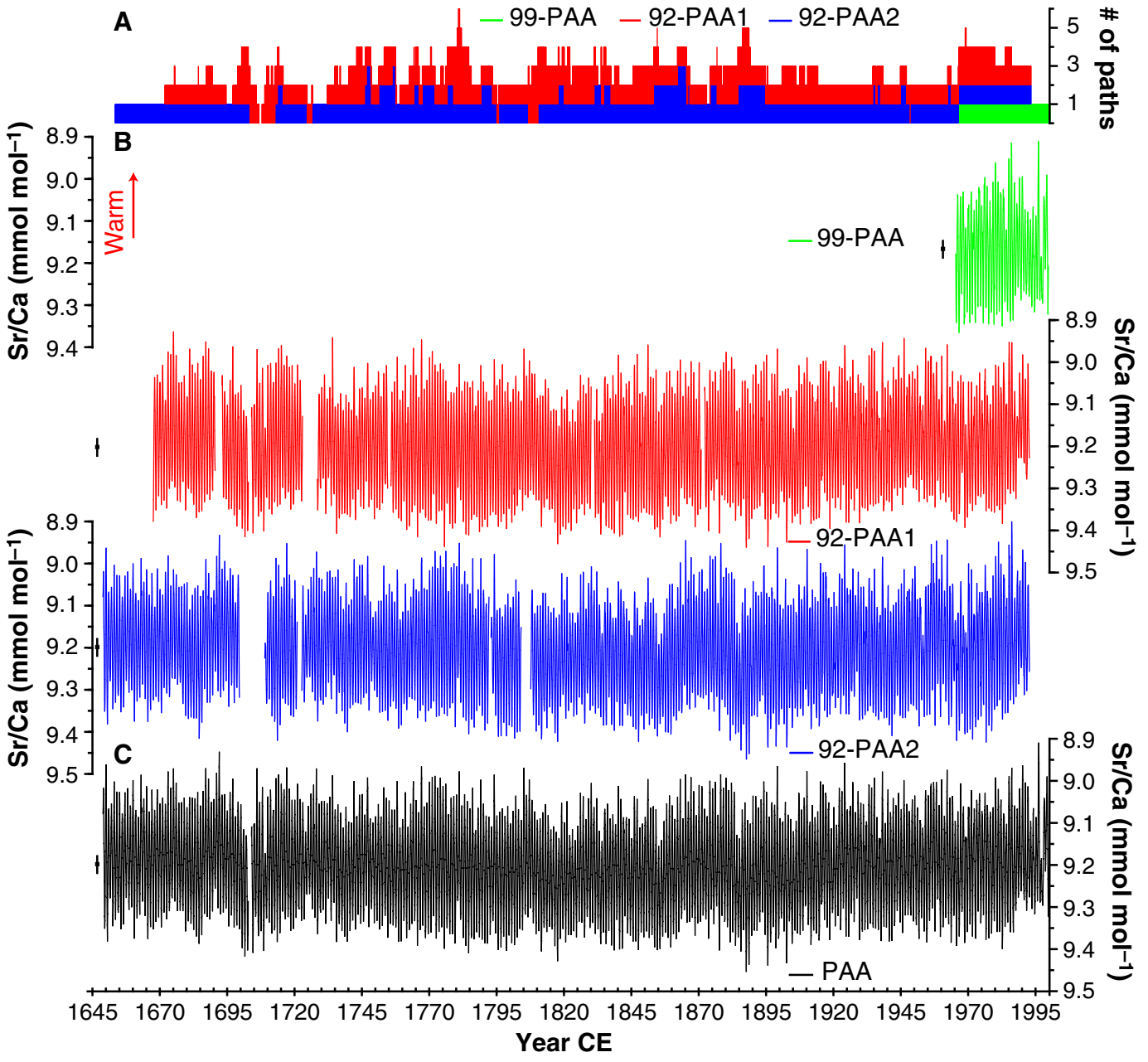

Fig. 3. The intracolony coral Sr/Ca variations. (a) Number (#) of paths sampled for each month. (b) Monthly coral Sr/Ca variations for cores 99-PAA, 92-PAA1, and 92-PAA2, which are described in this study and previous studies (Stephans et al., 2004; DeLong et al., 2007). Each core time series is the average of the coral Sr/Ca variations from contemporaneous paths. (c) PAA is the average of the intracolony coral Sr/Ca time series in (b). Sr/Ca axes are reversed so that warmer values (i.e., lower Sr/Ca values) are up. Error bars represent analytical precision (2σ).

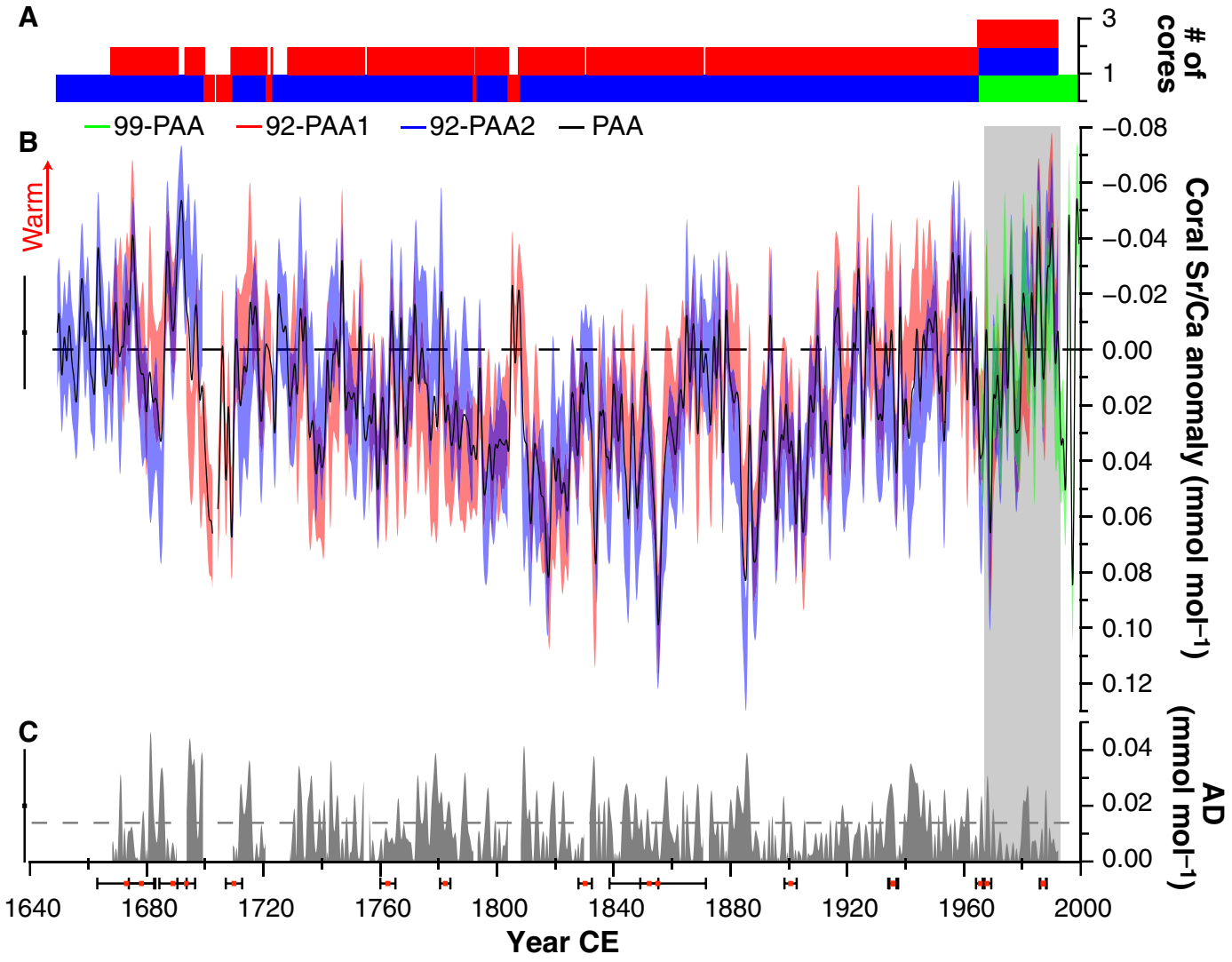

Fig. 4. Interannual coral Sr/Ca reproducibility. (a) Number of cores sampled for each month. (b) Monthly coral Sr/Ca anomalies smoothed with a 24-month LPFIR filter (90% pass = 40 months) (Bloomfield, 2000) to minimize subannual dating uncertainties. Shaded areas and error bars represent analytical precision (2σ). PAA is the average of 99-PAA, 92-PAA1, and 92-PAA2. Anomalies calculated with respect to the interval from 1967 to 1992 CE (vertical gray box), the common interval for the coral cores with IRD SST. Correlation between these time series is significant ($r = 0.65$; $n = 3496$, and $p < 0.001$). (c) Absolute differences (AD; Eq. (1)) determined between 92-PAA1 and 92-PAA2 (b) for any single month with gray dashed line denoting the mean (0.013 ± 0.009 mmol mol^{-1}, 1σ). Red boxes indicate ^{230}Th dates ±1σ analytical precision (Table 5).

<7 mm year^{-1}. These extension rates are "apparent" because the corallites are not parallel to the slab thus the distance between density bands is not true linear extension (Barnes et al., 1989; Lough and Barnes, 1990; Barnes and Lough, 1993). Merging or terminating corallite fans have cold biases in coral Sr/Ca (−0.65 to −1.77 °C; Table 2), which are associated with corallite growth ceasing (e.g., 92-PAA1-D in Fig. 1 and 92-PAA2-L in Fig. 2). A small corallite fan without optimal orientation (60 to 90 mm; Fig. 6d) has no discernable annual cycle in coral Sr/Ca and a shift from higher values to lower values. Disorganized corallites occurring near cavities and bioerosional incursions (e.g., 92-PAA1 core sections F1, J, H and I in Fig. 1) and are associated with indistinct density bands and a reduction in the apparent linear extension (3.6 to 6.7 mm year^{-1}; Table 2). Most disorganized corallites are detectable in X-radiographs; however, we identified a cold bias for the interval from 1662 to 1671 CE in 92-PAA2-M (Figs. 2, 7 and Table 2) that has clear density bands. Our examination of the slab surface reveals this path is between two small merging corallite fans not evident in the X-radiograph.

There are exceptions to our observation that suboptimal corallites tend to be warmer and disorganized corallites tend to be colder (Fig. 7 and Table 2). In 92-PAA2-D, the corallite fan appears normal in the X-radiograph; however, the corallites are not parallel to the slab surface with the resulting coral Sr/Ca determinations failing to capture the summer minima producing a cold bias. These samples are from the top of the core section with a small gap between sections making it difficult to discern corallite fan direction and size from this section alone. Examination of the bottom of 92-PAA2-C reveals this corallite fan is terminating (Fig. 2). We sampled a new path along an adjacent fan and these variations agree with synchronous coral Sr/Ca determinations in 92-PAA1. Core section 92-PAA1-J has suboptimal corallite alignment with higher Sr/Ca values (~1.94 °C colder); however, this core section and the prior section has bioerosional cavities and X-radiographs reveals disrupted growth (Fig. 1). From these examples, anomalies related disorganized corallites appear to dominate over suboptimal orientation. Furthermore, it is possible that the suboptimal sampling path transects the winter interval of the rotated time axis. We conducted a test on opposing sides of a core section with corallites perpendicular to the slab surface (1907 to 1908 CE on 92-PAA1-D; ~5 mm apart) and we found no difference in the coral Sr/Ca variations. The converse example is the core section 92-PAA2-G from 1804 to 1807 CE. We had difficulty

finding a good sampling path since the growth structures are small meandering corallite fans. We tried a path along the apex of one the small fans, which had optimal corallite orientation with acceptable extension (6.2 to 8.1 mm year^{-1}); however, the coral Sr/Ca determinations exhibited warmer winters (~3 °C) and summers (1.6 °C) with a reduced seasonal cycle (~1 °C) producing a large warm anomaly (1.85 °C, Fig. 7). A comparison with the contemporaneous and optimally sampled paths in the core 92-PAA1 reveals a warm period with less magnitude (Fig. 7). The path we selected failed to capture winter extremes in coral Sr/Ca presumably because more growth occurred in the summer associated with a new corallite fan. We decided to not include this path in the final reconstruction.

4.2. Sampling orientation with respect to the colony

We assess coral Sr/Ca reproducibility for optimal sampling paths with varying orientation (0°, 25°, 85°, and 90° with respect to the vertical axis) in a small *Porites lutea* colony (Fig. 8 and Table 4). The average linear extension for the paths is ~20 mm year^{-1} except for the path 85° from vertical (16.1 mm year^{-1}). Contemporaneous coral Sr/Ca variations agree within analytical precision regardless of orientation or sampling resolution (*t*-test, $p = 0.40$ to 0.84; f-test, $p = 0.06$ to 0.77). Annual averages determined from these sampling paths are approximately the same, even though we used different sampling resolutions, except for the vertical path, which is a shorter path. In the longer cores 92-PAA1

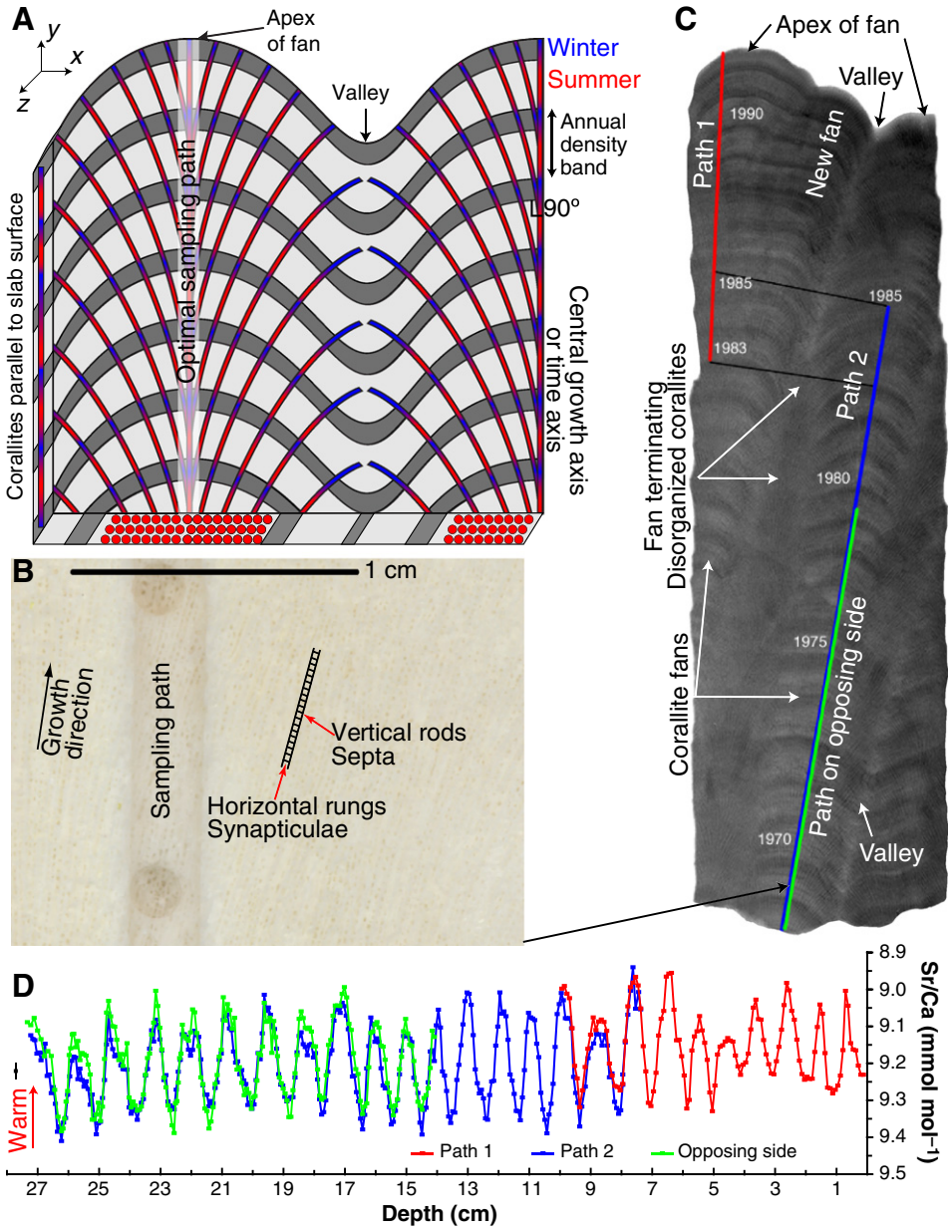

Fig. 5. Optimal sampling paths for massive *Porites* spp. (a) An illustration of a slab with new corallites forming along the apex of the corallite fan (*y*-axis) and extending upwards and outwards, similar to a feather duster, and terminating in the valley between fans. Shown here is the medial transect of the corallite fan that is parallel to the slab surface (*x*–*y* plane) with corallite growth direction perpendicular to the annual density bands or time axis in the corallum. The optimal sampling path is along the fan's central axis (*y*-axis). (b) The slab surface magnified to reveal extending corallites parallel to the slab surface with the vertical septa "rods" and horizontal synapticulae "rungs", which resemble a ladder. These parallel corallites are an example of the desired corallite orientation for optimal sampling. (c) X-radiograph of the core section 92-PAA1-A revealing annual density bands, extending corallite fans, apexes, and valleys. The sampling paths are along the approximate central axis of the corallite fans and corallites septa are parallel to the slab surface. (d) Coral Sr/Ca determinations from the optimal sampling paths in (c). We aligned the initial depth of each path to the preceding path. Note: the depth domain is not an exact representation of the time domain thus samples at the same depth (mm) may not be contemporaneous. Error bars represent analytical precision (2σ).
Adapted from Darke and Barnes, 1993.

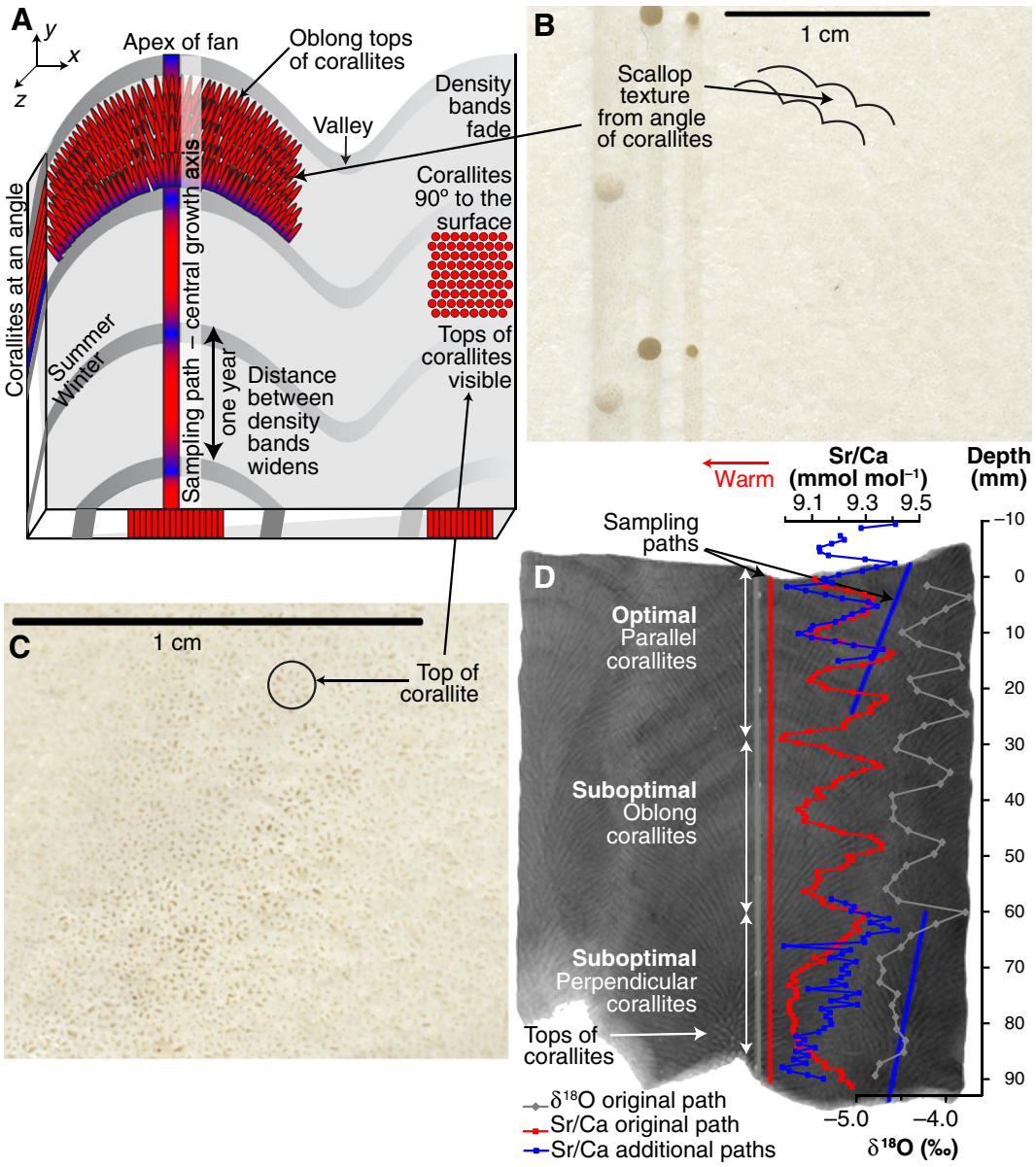

Fig. 6. Examples of suboptimal sampling in *Porites* spp. (a) Same as Fig. 5a with suboptimal corallite orientation (*z*-axis) relative to the slab surface (*x*–*y* plane). The left side illustrates a coral slab in which the corallites are at an angle (<90°) in the depth (*z*) direction with the corallites extending through the slab surface (*x*–*y* plane) in a oblong transect, which results in a scallop-edge texture on the slab surface (b). The feather-like formation of the corallite fan and the ladders are not visible on the slab surface (compare to Fig. 5c). The right side of (a) illustrates corallite orientation at 90° (*z*-axis) with respect to the slab surface (*x*–*y* plane) or radial transects in which the circular tops of the corallite calices are visible (c). (d) An example of suboptimal sampling from the core section 92-PAA1-K with coral Sr/Ca (red and blue; this study) and coral $\delta^{18}O$ (gray; Quinn et al., 1998) determinations superimposed on the X-radiograph parallel to the sampling paths (red, blue and gray lines, respectively).

and 92-PAA2, our optimal paths include those more than 30° from vertical (92-PAA1-F1, 92-PAA1-G2, and 92-PAA2-I; Figs. 1 and 2) with extension rates greater than 5.6 mm year^{-1}. These paths agree within 2σ of analytical precision with contemporaneous vertical paths in the same core and the other core (Figs. 3 and 4).

4.3. Chronology

Our chronology from cross dating two intracolony cores agrees with the ^{230}Th dates within analytical precision (Fig. 9 and Table 5). A previous study demonstrated site-specific initial ^{230}Th/^{232}Th (^{230}Th/^{232}Th$_{initial}$) values should be used for accurate ^{230}Th age calculation for shallow-water corals (Shen et al., 2008). Corrected ^{230}Th ages are calculated using a ^{230}Th/^{232}Th$_{initial}$ atomic ratio of 6.5×10^{-6} with an arbitrary 2σ variability of 20%, estimated by matching the corrected ^{230}Th age of the annual density band layer in 92-PAA1-H with a high ^{232}Th content of 3575 ± 12 parts per trillion (ppt) to its density band age. There is no significant difference between corrected ages of seven duplicate analyses with various ^{232}Th levels (10 to 1000 ppt) for seven layers, which verifies the well-estimated ^{230}Th/^{232}Th$_{initial}$ ratio. Precision of determined dates for all depths ranges from 1 to 4 years.

Cross dating the intracolony cores allows us to assess missing years in core breaks (Table 6). We find no missing years for core sections where the slabs fit together perfectly (e.g., 92-PAA1-F1 and 92-PAA1-F2 in Fig. 1) and 0 to 13 months missing along continuous sampling paths between core sections without a tight fit (e.g., 92-PAA1-L and 92-PAA1-K in Fig. 1). Core breaks with evidence of grinding between core sections have 0 to 30 months missing depending on the sample path selection (e.g., 92-PAA1-N and 92-PAA1-O in Fig. 1 and top of 92-PAA2-K in Fig. 2). Gaps of 3 to 9 years occur between core

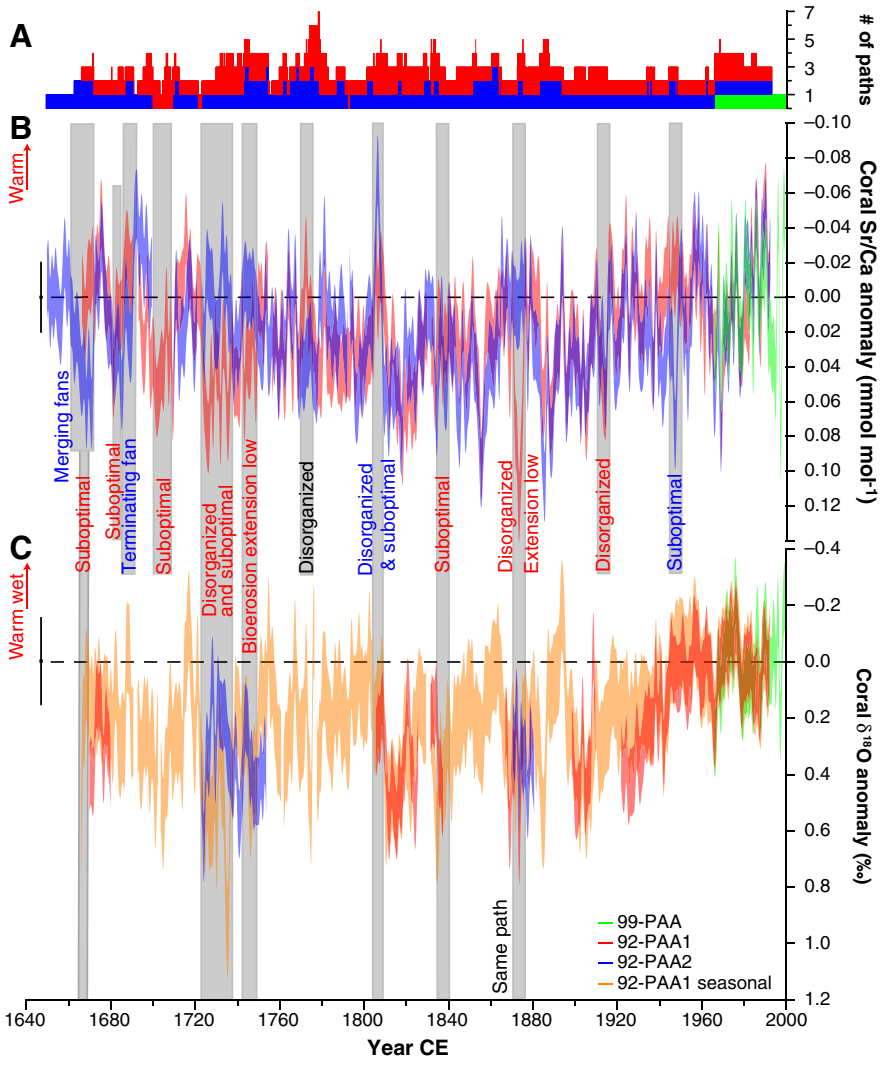

Fig. 7. Intracolony coral Sr/Ca reproducibility with suboptimal intervals included. (a) Number (#) of paths sampled. (b) Monthly coral Sr/Ca anomalies and (c) monthly (this study) and seasonal coral $\delta^{18}O$ anomalies (Quinn et al., 1998) same as Fig. 4 except problematic paths are included (gray boxes) with labels noting the type of sampling problem (Sections 4.1 and 5.1). We adjusted the seasonal coral $\delta^{18}O$ time series to the chronology presented here.

sections with disorganized corallites and obscure density bands in the X-radiographs (e.g., top of 92-PAA2-L in Fig. 2). Overall, the loss of time in both cores is ≤14 months back to 1728 CE. Before 1728 CE, the cores are staggered with gaps of 30 to 111 months with sclerochronology dates verified by three ^{230}Th dates (Figs. 4 and 9). We find core bottom dates of 1667 CE for 92-PAA1 and 1649 CE for 92-PAA2.

5. Discussion

There are different sources of anomalous coral Sr/Ca and $\delta^{18}O$ determinations, most result in higher coral Sr/Ca and $\delta^{18}O$ values whereas a few sources produce lower values. Higher than expected coral Sr/Ca and $\delta^{18}O$ determinations (i.e., colder temperatures) could be the result of slow growth rates (i.e., kinetic effects) (McConnaughey, 1989; de Villiers et al., 1994), thermal stress and bleaching (Marshall and McCulloch, 2002), marine secondary aragonite precipitation (Quinn and Taylor, 2006; Hendy et al., 2007), sampling in a valley between corallite fans (Alibert and McCulloch, 1997; Cohen and Hart, 1997), and disorganized corallite fans. Anomalously low coral Sr/Ca and $\delta^{18}O$ determinations (i.e., higher temperatures) result from secondary calcite precipitation (McGregor and Gagan, 2003) and suboptimal corallites. The annual cycles in geochemistry are altered or disappear with diagenesis (Quinn and Taylor, 2006) and with thermal stress from bleaching (Marshall and McCulloch, 2002) whereas the cycles may still be evident with reduced growth, suboptimal and disorganized sampling. Here we discuss anomalous coral Sr/Ca and $\delta^{18}O$ determinations related to sample path selection and how these anomalies manifest as 1) sampling uncertainties, and 2) chronology discrepancies as well as the implications for coral-based climate reconstructions. Sampling path selection may produce discrepancies in other geochemical proxies from coral skeletons or measurements of the corallum yet these remain to be evaluated. The other sources of uncertainties and discrepancies in coral records, such as environmental, diagenesis, thermal stress, and biological processes, will not be discussed further (see Corrège, 2006; Jones et al., 2009; DeLong et al., 2010, 2011; Lough and Cooper, 2011).

5.1. Sampling uncertainties

The sampling biases documented in this study can be subtle to large and span several years with clear annual cycles, thus appear to be real temperature variability (Fig. 7 and Table 2). Suboptimal alignment of corallites is particularly problematic because it can occur along the major growth axis and is not readily apparent in X-radiographs (Fig. 6; Fig. 5 in DeLong et al. (2007)). The analysis by Lough and Barnes (1990) finds an average of 2 mm displacement on opposing sides of a 6 to 7 mm slab, thus sampling along the major growth axis evident in the X-radiograph may produce different geochemical time series on

Table 2
Summary of sampling issues detected.

Core section	Year [a]	Type	Proxy	Bias (°C) [b]	Extension [c]	Notes
92-PAA1-B	1960–1965	Suboptimal	Sr/Ca	+1.77 (n=67)	11.9 (n=7)	Corallites at angle to the slab surface.
				+1.67 (n=67)		
			$\delta^{18}O$	+0.16 (n=48)		
92-PAA1-D	1912–1914	Disorganize	Sr/Ca	−0.87 (n=26)	14.0 (n=2)	Merging fans and reduced annual cycle.
				−0.65 (n=26)		
92-PAA1-D	1907–1908	Suboptimal		+0.04 (n=13)	22.0 (n=1)	Corallites at 90° with respect to slab surface. False year.
				+0.19 (n=13)		
92-PAA1-F1	1870–1875	Disorganize	Sr/Ca	−2.40 (n=44)	7.7 (n=5)	Reduced extension (lowest=3.5 mm) and annual cycle. Cavity in coral (Fig. 1).
				−2.45 (n=57)	5.1 (n=3)	
92-PAA1-F2	1831–1836	Suboptimal	Sr/Ca	+0.83 (n=61)	11.5 (n=5)	Corallites at angle to the slab surface.
				+0.53 (n=61)		
			$\delta^{18}O$	−0.36 (n=20)		
92-PAA1-L	1772–1776	Disorganize		+0.44 (n=56)	8.1 (n=5)	Reduced annual cycle and no seasonal extremes.
				−0.11 (n=56)	6.3 (n=1)	
92-PAA1-K	1755–1754	Suboptimal	Sr/Ca	NA	22.4 (n=3)	Corallites at 90° with respect to slab surface.
				+2.30 (n=15)	40.6 (n=1)	
92-PAA1-J	1742–1749	Disorganize	Sr/Ca	−0.76 (n=90)	4.9 (n=2)	Reduced apparent extension, cavity, and did not capture summer minima.
				−1.06 (n=90)	4.9 (n=2)	
			$\delta^{18}O$	NA		
				+0.02 (n=90)		
92-PAA1-J	1734–1736	Suboptimal	Sr/Ca	−1.41 (n=29)	14.7 (n=1)	Corallites rotating to 90° with respect to slab surface and reduced
		disorganize		−1.94 (n=29)	7.7 (n=1)	annual cycle. This core section and prior interval has bioerosion (Fig. 1).
			$\delta^{18}O$	NA		
				−1.05 (n=10)		
92-PAA1-I	1731–1737	Disorganize	Sr/Ca	−0.52 (n=77)	4.7 (n=6)	Reduced apparent extension, cavity, no summer maxima,
		suboptimal		−1.02 (n=77)	2.1 (n=1)	and false years. This core section and prior interval has bioerosion (Fig. 1).
			$\delta^{18}O$	NA		
				−0.61 (n=14)		
92-PAA1-H	1723–1732	Disorganize	Sr/Ca	NA	4.6 (n=9)	Reduced apparent extension, cavity, and no summer minima. Cavity in coral (Fig. 1).
		suboptimal		−0.98 (n=100)	3.6 (n=1)	
92-PAA1-M	1701–1707	Suboptimal		+0.14 (n=67)	12.9 (n=6)	Corallites rotating to 90° with respect to slab surface. False years.
				NA	21.7 (n=1)	
92-PAA1-M	1692–1693	Suboptimal		NA	13.9 (n=1)	Corallites rotating to 90° with respect to slab surface.
				+0.04 (n=9)		
92-PAA1-O	1680–1681	Disorganize	Sr/Ca	−0.23 (n=17)	6.0 (n=1)	Corallites at angle and no summer minima.
				−0.12 (n=17)		
92-PAA1-O	1665–1667	Suboptimal	Sr/Ca	NA	13.7 (n=2)	Corallites rotating to 90° with respect to slab surface and no winter extremes.
				+0.11 (n=24)	15.3 (n=1)	
92-PAA2-D	1945–1948	Disorganize	Sr/Ca	−1.86 (n=27)	7.5 (n=1)	Reduced annual cycle and no summer minima.
		suboptimal		−2.42 (n=27)		
92-PAA2-G	1800–1807	Disorganize	Sr/Ca	NA	7.0 (n=6)	Reduced annual cycle, and small fans.
		suboptimal		+0.61 (n=82)	6.4 (n=1)	
92-PAA2-H	1772–1778	Disorganize	Sr/Ca	−1.65 (n=75)	8.3 (n=45	Reduced annual cycle, merging fans and valley.
				−1.14 (n=75)	6.7 (n=1)	
92-PAA2-I	1766–1772	Disorganize	Sr/Ca	−1.40 (n=56)	7.7 (n=4)	Reduced annual cycle and merging fans.
				−1.23 (n=56)	5.9 (n=1)	
92-PAA2-I	1744–1747	Disorganize	Sr/Ca	−0.35 (n=36)	6.3 (n=4)	Reduced annual cycle, reduced extension, small and merging fans.
		suboptimal		−0.22 (n=36)	5.8 (n=1)	
92-PAA2-L	1699–1709	Disorganize		No samples		No optimal paths, gap between sections.
92-PAA2-L	1686–1690	Disorganize	Sr/Ca	−1.24 (n=50)	8.3 (n=4)	Terminating fan.
				−1.23 (n=50)	5.4 (n=1)	
92-PAA2-M	1662–1671	Disorganize	Sr/Ca	−1.70 (n=110)	8.6 (n=9)	Merging fans.
				−1.77 (n=110)		

[a] Chronology from this study. Years are CE.
[b] With respect to samples with optimal orientation from either the same core (first value) or the other core from the same colony (second value), with no comparison available noted with NA (not available). Values are given for coral $\delta^{18}O$ if available. Biases are determined in the time domain and are reported with number of observations (n). Average bias for the interval are reported as degrees Celsius using the transfer function 0.054 mmol mol^{-1} °C^{-1} for coral Sr/Ca (DeLong et al., 2007) and 0.22‰ °C^{-1} for coral $\delta^{18}O$.
[c] Average apparent extension per year determined from geochemical variations. Units are mm year^{-1}. Values with n=1 are either a minimum or maximum.

Table 3
Average geochemistry from 92-PAA1-K for optimal and suboptimal paths.

Depth (mm)	Sr/Ca depth domain (mmol mol^{-1})	Sr/Ca time domain [a] (mmol mol^{-1})	Sr/Ca 92-PAA2 [b] (mmol mol^{-1})	$\delta^{18}O$ [c] depth domain (‰ VPDB)	$\delta^{18}O$ [c] time domain [a] (‰ VPDB)
0.0 to 29.0	9.224±0.108	9.225±0.093	9.226±0.089	−4.13±0.27	−4.11±0.24
Optimal	(n=42)	(n=35)	(n=35)	(n=14)	(n=11)
29.1 to 60.5	9.186±0.093	9.200±0.100	9.197±0.093	−4.34±0.29	−4.32±0.29
Suboptimal <90°	(n=45)	(n=29)	(n=29)	(n=15)	(n=11)
60.6 to 92.0	9.115±0.090	9.114±0.089	9.240±0.102	−4.56±0.18	−4.60±0.16
Suboptimal 90°	(n=44)	(n=24)	(n=15)	(n=14)	(n=6)

[a] Depth domain data was converted to time domain and linearly interpolated to even monthly intervals.
[b] Contemporaneous coral Sr/Ca averages from 92-PAA2-I.
[c] Contemporaneous coral $\delta^{18}O$ averages from 92-PAA1-K reported by Quinn et al. (1998) for which the sampling interval is ~4 samples year^{-1}. Depth domain data were converted to time domain and linearly interpolated to an even 4 samples year^{-1}.

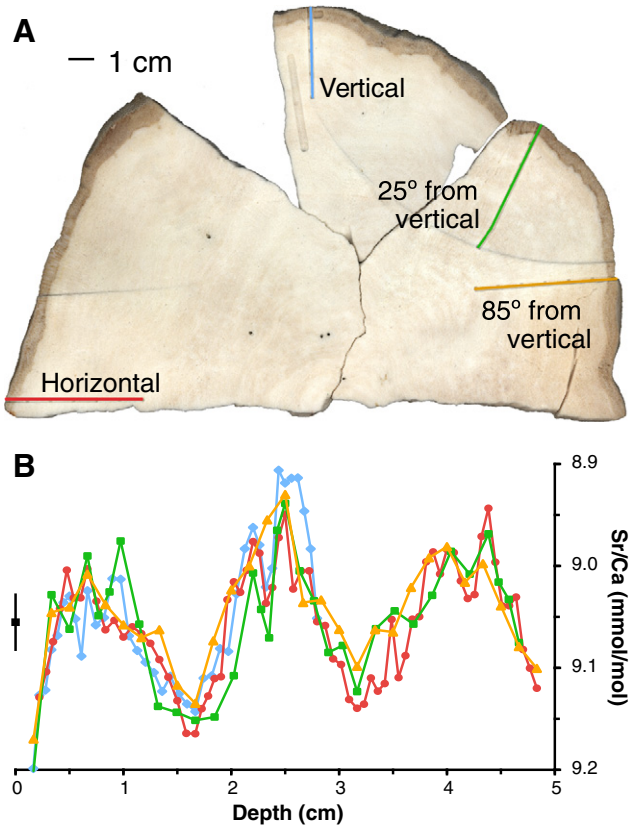

Fig. 8. Sampling orientation with respect to the colony. (a) Vertical cross section of a small *Porites lutea* colony from Vanuatu with sampling paths at various angles from vertical axis of the colony. Sampling paths have optimal corallite alignment with respect to the slab surface. (b) Coral Sr/Ca determinations for the sampling paths in (a) with colors matching the labels in (a). Depth from each core was aligned to the path 85° from vertical for comparison (Table 4). Error bar represents analytical precision (2σ).

opposing sides of a slab (DeLong et al., 2007). There are indicators of suboptimal orientation in X-radiographs such as indistinct banding patterns and longer than average distance between high-density bands (Fig. 6). Examining the centimeter-scale growth patterns around the sampling track can give clues to corallite orientation. If there is an area with corallites at 90° to the surface, then there is a transition area from parallel to perpendicular corallites. Our examination of coral X-radiographs reveals perpendicular corallites can form and disappear quickly producing short-lived warm periods, which could be interpreted as real climatic events and as false years (e.g., 1907 to 1909 CE in 92-PAA1-D in Fig. 1). The direction of the corallites can change on the centimeter scale but this suboptimal bias can be avoided by examining the slab surface under low power magnification during sample path selection.

Suboptimal orientation is problematic for studies using bulk sampling with annual intervals or longer, such as 5-year intervals. These studies assume that coral growth is constant thus their sampling interval represents an average; however, this may not be true for all coral species and may vary between individual colonies (Barnes et al., 1995; Gagan et al., 2012). In the coral colony examined, suboptimal intervals along the slab surface have elongated years with more summer samples in the season with more growth resulting in a warm bias relative to synchronous samples with optimal orientation. We find that this bias is reduced by converting approximately monthly samples from the depth domain to the time domain using four alignment points per year and linearly interpolating to even monthly intervals. For example, the average coral Sr/Ca for the optimal interval in 92-PAA1-K (0 to 29 mm; Fig. 6 and Table 3) in the depth and time domain are approximately the same, for which the depth domain represents bulk sampling and the time domain is monthly samples interpolated to even time steps. In the interval with suboptimal corallites (29.1 to 50.6 mm), the averages between the depth and time domain differ by 0.014 mmol mol^{-1} (or 0.26 °C) with 16 more samples in the bulk average. The time domain average is approximately the same as the optimal path from 92-PAA2. For interval with perpendicular corallites (60.6 to 92.0 mm), the averages are approximately the same between the depth and time domain but are lower than the average coral Sr/Ca from the optimally sampled 92-PAA2 (0.125 mmol mol^{-1} or 2.30 °C warmer than 92-PAA2). The averages for seasonal coral $\delta^{18}O$ are the same between depth and time domain suggesting that the bias is not removed; however, a shift to more negative $\delta^{18}O$ values occurs with increasing rotation of the corallites

Table 4
Summary of coral Sr/Ca from sampling paths at different angles within a colony[a].

Statistic	Vertical	25°	85°	Horizontal
Mean	9.048	9.052	9.045	9.055
Median	9.055	9.044	9.040	9.052
Standard deviation	0.071	0.061	0.052	0.055
Maximum	9.199	9.201	9.170	9.165
Minimum	8.906	8.939	8.930	8.943
Annual average [b]	9.007 ± 0.075	9.056 ± 0.016	9.051 ± 0.023	9.047 ± 0.024
n [c]	40	33	29	69
Extension [d]	19.8 ± 0.9	20.0 ± 1.7	16.1 ± 1.0	19.9 ± 0.16
Sampling [e]	0.83	1.67	1.67	0.83

[a] Determined in depth domain from 0 to 5 cm except for vertical, determinations were made for 0 to 2.8 cm (Fig. 8). Units are mmol mol^{-1} unless otherwise indicated.
[b] Number of years for mean annual average (±1σ) is three except for vertical for which only two incomplete years are sampled. Additionally, the last year may not have captured winter maxima in coral Sr/Ca (Fig. 8).
[c] Number of observations (*n*) for each path.
[d] Determine between winter maxima (August) in Sr/Ca for each year. Units are mm $year^{-1}$ and reported as an average ±1 standard deviation.
[e] Sampling interval (mm $sample^{-1}$) for each path.

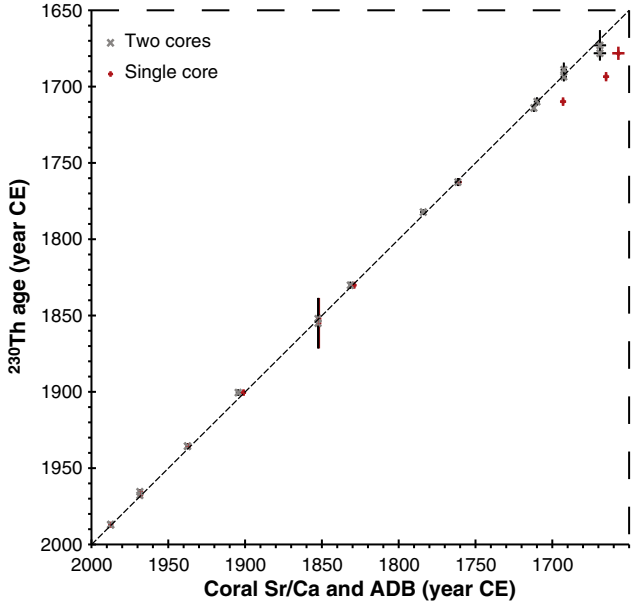

Fig. 9. Comparison of sclerochronology dates with ^{230}Th dates. Sclerochronology determined by cross-dating coral Sr/Ca variations from two cores (92-PAA1 and 92-PAA2) and counting annual density bands (ADB). Samples for ^{230}Th dating were extracted from the core 92-PAA1 (Fig. 1 and Table 5). Error bars for ^{230}Th dates represent analytical precision (2σ). Error bars for sclerochronology method were determined by examining ^{230}Th sample area in X-radiographs (e.g., sample contains ~1 ± 0.5 year; Fig. 1). For the single core dates (red), the sclerochronology date of the ^{230}Th samples is from the chronology determined by the previous study (Quinn et al., 1998).

Table 5
Uranium and thorium isotopic compositions and ^{230}Th ages for corals determined by ICP-MS.

Core ID	^{238}U (ppb)	^{232}Th (ppt)	δ^{234}U Measured [a]	[^{230}Th/^{238}U] Activity [b]	[^{230}Th/^{232}Th] (ppm) [c]	Age Uncorrected	Age Corrected [b, d]	^{230}Th date CE	$\delta^{234}U_{initial}$ Corrected [e]	Sr/Ca-ADB Year CE [f]
92-PAA1-A	3028.3 ± 5.7	318.7 ± 1.4	145.3 ± 2.1	0.0002367 ± 0.0000075	37.1 ± 1.2	22.57 ± 0.72	18.6 ± 1.1	1986.9 ± 1.1	145.3 ± 2.1	1987.5 ± 0.5
92-PAA1-A*	2931.1 ± 6.7	18.89 ± 0.60	148.5 ± 2.3	0.000196 ± 0.000012	502 ± 33	18.6 ± 1.1	18.4 ± 1.1	1987.1 ± 1.1	148.5 ± 2.3	1987.5 ± 0.5
92-PAA1-B	2771.9 ± 4.5	426.8 ± 1.6	146.3 ± 1.9	0.000457 ± 0.000010	49.0 ± 1.0	43.54 ± 0.92	37.8 ± 1.5	1967.8 ± 1.5	146.3 ± 1.9	1968.5 ± 0.5
92-PAA1-B*	2814.8 ± 6.7	53.4 ± 1.0	145.5 ± 2.7	0.000428 ± 0.000015	372 ± 15	40.8 ± 1.5	40.1 ± 1.5	1965.5 ± 1.5	145.5 ± 2.7	1968.5 ± 0.5
92-PAA1-C	2794.6 ± 4.6	341.4 ± 1.2	145.9 ± 1.7	0.000782 ± 0.000008	105.7 ± 1.2	74.55 ± 0.81	70.0 ± 1.2	1935.6 ± 1.2	145.9 ± 1.7	1937.5 ± 0.5
92-PAA1-C*	2731.0 ± 7.3	20.33 ± 0.79	145.8 ± 2.9	0.000736 ± 0.000018	1632 ± 75	70.2 ± 1.7	69.9 ± 1.7	1935.6 ± 1.7	145.8 ± 2.9	1937.5 ± 0.5
92-PAA1-E	3022.9 ± 8.8	39.29 ± 0.64	145.1 ± 2.9	0.001106 ± 0.000022	1405 ± 36	105.5 ± 2.1	105.0 ± 2.1	1900.5 ± 2.1	145.2 ± 2.9	1904.5 ± 0.8
92-PAA1-F1	2912.5 ± 7.5	19.78 ± 0.69	144.9 ± 2.8	0.001610 ± 0.000032	3914 ± 156	153.7 ± 3.1	153.4 ± 3.1	1852.1 ± 3.1	144.9 ± 2.8	1852.5 ± 0.5
92-PAA1-F1*	2906.0 ± 5.6	6203 ± 18	146.5 ± 2.0	0.002419 ± 0.000042	18.71 ± 0.33	230.6 ± 4.1	150 ± 17	1855 ± 17	146.5 ± 2.0	1852.5 ± 0.5
92-PAA1-F2	2870.4 ± 6.2	589.1 ± 1.8	144.0 ± 2.2	0.001917 ± 0.000018	154.2 ± 1.5	183.1 ± 1.7	175.4 ± 2.3	1830.1 ± 2.3	144.1 ± 2.2	1831.5 ± 0.5
92-PAA1-G2	2887.4 ± 5.2	271.36 ± 0.89	145.2 ± 2.0	0.002377 ± 0.000016	417.6 ± 3.1	226.9 ± 1.6	223.3 ± 1.8	1782.2 ± 1.8	145.3 ± 2.0	1784.0 ± 1.0
92-PAA1-K	2913.9 ± 6.2	736.7 ± 1.7	146.4 ± 2.3	0.002648 ± 0.000018	172.9 ± 1.2	252.5 ± 1.8	243.0 ± 2.6	1762.6 ± 2.6	146.5 ± 2.3	1761.5 ± 1.0
92-PAA1-H	2858.5 ± 8.1	3575 ± 12	148.0 ± 2.5	0.003470 ± 0.000047	45.80 ± 0.62	330.5 ± 4.5		1710[d]	148.4 ± 1.5	1710.0 ± 1.0
92-PAA1-H†	2713.6 ± 4.8	169.2 ± 3.8	148.2 ± 2.7	0.003103 ± 0.000044	822 ± 22	295.5 ± 4.2	293.1 ± 4.2		148.3 ± 2.7	1712.0 ± 2.0
92-PAA1-H†*	2845.6 ± 5.1	308.7 ± 3.5	149.1 ± 2.8	0.003154 ± 0.000047	480.0 ± 8.9	300.1 ± 4.5	296.0 ± 4.6		149.3 ± 2.8	1712.0 ± 2.0
92-PAA1-H†*	2746.9 ± 4.7	141.9 ± 3.3	147.5 ± 2.6	0.003129 ± 0.000048	1000 ± 28	298.2 ± 4.7	296.2 ± 4.7		147.6 ± 2.6	1712.0 ± 2.0
						wt-average age	295.0 ± 2.6	1714.0 ± 2.6		
92-PAA1-M	2870.4 ± 6.5	762.2 ± 1.6	144.9 ± 2.2	0.003371 ± 0.000023	209.6 ± 1.4	322.0 ± 2.3	312.0 ± 3.0	1693.5 ± 3.0	145.1 ± 2.2	1692.5 ± 1.0
92-PAA1-M*	2775.2 ± 5.1	14.7 ± 1.1	144.6 ± 2.4	0.003316 ± 0.000048	10,357 ± 757	316.8 ± 4.7	316.6 ± 4.7	1689.0 ± 4.7	144.7 ± 2.4	1692.5 ± 1.0
92-PAA1-O	2933.2 ± 6.1	1371.9 ± 4.2	145.0 ± 1.9	0.003611 ± 0.000026	127.5 ± 1.0	344.9 ± 2.5	327.4 ± 4.3	1678.2 ± 4.3	145.1 ± 2.0	1669.0 ± 2.0
92-PAA1-O*	2912.0 ± 5.4	23.9 ± 1.0	142.7 ± 2.4	0.00348 ± 0.00010	7009 ± 348	332.9 ± 9.9	332.6 ± 9.9	1673.0 ± 9.9	142.9 ± 2.4	1669.0 ± 2.0

Analytical errors are 2σ of the mean. Years are Common Era (CE).

[a] $\delta^{234}U = ([^{234}U/^{238}U]_{activity} - 1) \times 1000$.

[b] $[^{230}Th/^{238}U]_{activity} = 1 - e^{-\lambda 230 T} + (\delta^{234}U_{measured}/1000)[\lambda_{230}/(\lambda_{230} - \lambda_{234})](1 - e^{-(\lambda 230 - \lambda 234)T})$, where T is corrected age. Decay constants are 9.1577×10^{-6} year^{-1} for ^{230}Th, 2.8263×10^{-6} year^{-1} for ^{234}U (Cheng et al., 2000) and 1.55125×10^{-10} year^{-1} for ^{238}U (Jaffey et al., 1971).

[c] The degree of detrital ^{230}Th contamination is indicated by the [^{230}Th/^{232}Th] atomic ratio instead of the activity ratio.

[d] Age corrections are calculated using a $^{230}Th/^{232}Th_{initial}$ ratio of $6.5 \pm 1.3 \times 10^{-6}$ estimated from layer 92-PAA1-H (Subsection 4.3).

[e] $\delta^{234}U_{initial}$ corrected is calculated based on ^{230}Th age (T), i.e., $\delta^{234}U_{initial} = \delta^{234}U_{measured}$ x $e^{\lambda 234 * T}$, and T is corrected age.

[f] Coral Sr/Ca and annual density band ages are determined by cross dating the cores 92-PAA1 and 92-PAA2 with uncertainty based on the estimated time interval of the sampling area in scanned images of the coral slabs compared with digital X-radiographs of those slabs (e.g., sample contains ~1 ± 0.5 year).

* Denotes duplicate subsamples.

† Denotes additional samples from the core section but two years younger than 92-PAA1-H (see Fig. 1).

but we do not have δ^{18}O determinations from 92-PAA2 to assess the magnitude of the bias.

An example from 92-PAA1-K illustrates that comparisons between studies using bulk or annual samples with studies using approximately monthly samples may not agree in intervals with suboptimal sampling. This may explain some of the differences in the coral Sr/Ca time series noted by Linsley et al. (2006) for records from Fiji and Rarotonga for which annual and monthly sampling resolutions were used. Our shallow water massive *Porites* colony grows more in the warm months (Fig. 5d) whereas other coral colonies or species may extend more at other times of the year; therefore, the suboptimal sampling bias may vary with coral colony, location, and species.

The cold bias classified as disorganized resembles the bias in coral Sr/Ca and δ^{18}O previously reported (see Introduction and Alibert and McCulloch, 1997; Cohen and Hart, 1997). Valleys between corallite fans are the result of corallite growth occluding with the corallites being compressed and their walls becoming thin and less dense (Darke and Barnes, 1993) yet linear extension may not be reduced (Alibert and McCulloch, 1997; Cohen and Hart, 1997). We also find that merging and terminating corallite fans in the X-radiographs are lighter or less dense compared to fans with active growth (Figs. 1, 2, 5 and 6). Calcification rate is the product of extension rate and density (Lough and Barnes, 1997); therefore, calcification rates are reduced in low density areas of the slab. Unfortunately, disorganized corallites

Table 6
Summary of missing time between core sections.

92-PAA1	Months [a]	Notes	92-PAA2	Months	Notes
A → B	0	Perfect fit between sections.	A → B	0	Perfect fit between sections.
B → C	0	Good fit between sections, slightly rotated.	B → C	0	Good fit between sections.
C → D	1	Good fit between sections, slightly rotated.	C → D	0	Grinding between sections used additional path for gap.
D → E	0	Good fit between sections with some grinding.	D → E	0	Good fit between sections used additional path for gap.
E → F1	0 (1)	Good fit between sections, and bioerosion.	E → F1	0	Good fit between sections used additional path for gap.
F1 → F2	0	Perfect fit between sections.	F1 → F2	0	Perfect fit between sections.
F2 → G1	13 (14)	Some fit, X-radiographs have continuous banding patterns.	F2 → G	0	Good fit between sections used additional path for gap.
G1 → G2	0	Perfect fit between sections.	G → H	8	Some fit, X-radiographs have continuous banding patterns.
G2 → L	0 (12)	Some fit between sections, used new paths to bridge gap.	H → I	0	Good fit between sections used overlapping paths.
L → K	0 (6)	Some grinding, used new paths to fill gap.	I → J	0	Good fit between sections continuous paths.
K → J	14	No fit between sections, 90° orientation at bottom of K.	J → K	19	Grinding between sections.
J → I	0 (8)	Grinding between sections used new paths to bridge gap.	K → L	111	Grinding and top of section L has disorganized corallites.
I → H	0	Some fit with grinding between sections and bioerosion.	L → M	0	Some fit between sections, X-radiographs has continuous banding patterns.
H → M	0	No fit with grinding between sections, paths overlap.			
M → N	30	Some fit but banding patterns are not continuous and corallites are disorganized at bottom of 92-PAA1-M.			
N → O	0	Heavy grinding between sections, paths overlap.			

[a] Number of months missing for the cross-dated chronology with additional paths included in this study. The number in parentheses is for just the paths used in the study of Quinn et al. (1998) if different.

do not have clear corallite growth structures on the slab surface and obscure density banding in the X-radiographs; therefore, extension and calcification rates cannot be determined. Kinetic effects from reduced calcification may explain the shift to higher coral Sr/Ca and $\delta^{18}O$ values (McConnaughey, 1989); however, kinetic effects do not explain all the biases observed (Table 2). Cohen and Hart (1997) suggest that shading on the centimeter scale between bumps and valleys on the colony surface reduces light-enhanced calcification producing a shift towards higher coral $\delta^{18}O$ values. We find that coral Sr/Ca is the same between horizontal and vertical sampling paths on large and small colonies (Section 5.2); therefore, shading effects on the centimeter scale are implausible.

Another study reports a lack of reproducibility for coral Sr/Ca variations between sampling paths in close proximity on separate corallite fans (Alibert and Kinsley, 2008). Our examination of their X-radiographs reveals problematic centimeter-scale structures such as suboptimal corallites, terminating corallite fans, and unclear density bands. For example, the interval from 1881 to 1883 CE appears to have corallites rotated with respect to the slab surface; however, suboptimal corallites are difficult to detect without examining the coral slab. Their path starting in 1868 CE is located at a termination of a corallite fan, thus the coral Sr/Ca determinations are colder than synchronous samples from an adjacent path. Those authors find the X-radiographs have low density and reduced extension rates associated with the terminating fan; they suggest this discrepancy is caused by lower calcification rates thus kinetic effects. They recommend and we concur that kinetic effects cannot be detected by extension rate alone. Extension rates are easy to determine and are regularly monitored, whereas density variations are harder to determine and to our knowledge no threshold values for low density have been determined. Furthermore, density varies between coral genera, thus density thresholds may vary as well.

Suboptimal and disorganized corallites can be problematic for reconstructions using a single core. For example, a previous reconstruction sampled the core 92-PAA1 (Corrège et al., 2001) and found a ~1.4 °C cooling in New Caledonia for the interval from 1701 to 1761 CE, a period within the Little Ice Age. That reconstruction examined coral Sr/Ca and U/Ca variations from core sections 92-PAA1-K, J, H, and I, which contain bioerosional cavities (Fig. 1). In order to replicate the previous reconstruction's results, we sampled 92-PAA1 adjacent to the paths used in previous reconstruction (Quinn et al., 1998; Corrège et al., 2001) (Fig. 1) and we sampled a second core, 92-PAA2, from the same colony, which had no cavities. Our coral Sr/Ca time series between these cores agree within analytical precision with some exceptions (Fig. 7 and Table 2). Examination of the coral slab for the intervals with discrepancies revealed disorganized corallites along the paths sampled by previous reconstruction, which resulted in colder temperatures (compare Figs. 4 and 7). We sampled new paths on 92-PAA1 with optimal corallite alignment and these new paths agreed with the second core (92-PAA2) within analytical precision. Our coral Sr/Ca-SST reconstruction has an average temperature departure of −0.19 °C (±0.57 °C, 1σ) for the interval from 1701 to 1761 CE (DeLong et al., 2012a), which agrees with the coral Sr/Ca-SST reconstruction from nearby Flinders Reef (−0.10±0.42 °C, 1σ) (Calvo et al., 2007). Preliminary analyses with monthly $\delta^{18}O$ from 92-PAA2 for this interval compared with seasonal $\delta^{18}O$ from 92-PAA1 (Quinn et al., 1998) reveal some discrepancies suggesting that disorganized corallites can affect coral $\delta^{18}O$ (Fig. 7).

5.2. Sampling orientation and extension rates

Our results for sampling orientation within a coral colony reveal no significant mean shifts in coral Sr/Ca determinations and these determinations are within analytical precision when optimal sampling is used for both large and small colonies with extension rates >5 mm year^{-1} (Figs. 3, 4, and 8). Comparable results for coral Sr/Ca are reported for a *Porites australiensis* colony (10 cm high) and a *Porites mayeri* colony (1.4 m high) between vertical and horizontal sampling paths with extension rates of >7 mm year^{-1} (Alibert and McCulloch, 1997; Mitsuguchi et al., 2003). Other studies find no significant difference for mean $\delta^{18}O$ determinations for *Porites* spp. from small, large, and microatoll colonies with growth rates >6 mm year^{-1} (Maier et al., 2004; Felis et al., 2009; McGregor et al., 2011).

Some studies suggest horizontal-sampling paths should be avoided due to possible growth-related effects (McConnaughey, 1989; de Villiers et al., 1994, 1995) whereas others suggest horizontal cores are more reliable for temperature reconstructions (Heiss et al., 1999; Cahyarini et al., 2009). One such study finds small differences in the average of coral $\delta^{18}O$ between vertical and horizontal transects (0.08‰, 0.10‰, respectively) with average growth rates between 14.8 and 12.2 mm year^{-1}, respectively, extracted from a large *Porites* colony (~4 m tall) (Heiss et al., 1999). Those authors find the difference between the oldest and youngest intervals of each transect are larger for the vertical transect (0.39‰ vs. 0.22‰) in which the top of the colony grew into shallower and warmer water whereas the horizontal core remained at a constant depth (~3.5 m difference in water depth). Those results and others suggest warming trends in multi-century temperature reconstructions from vertical cores may be related to the colony growing into shallower and warmer water (Heiss et al., 1999; Scott et al., 2010). However, our temperature reconstruction reveals a warm–cold–warm pattern for the past 350 years suggesting this is not the case with our colony or the effect is minimal (Fig. 4 and see Fig. 2 in DeLong et al. (2012a)). Another study with a large *Porites* colony (~2.4 m high), which the vertical surface had almost reached the sea surface, finds significant differences in mean coral Sr/Ca between horizontal and vertical cores in which the horizontal core had a higher correlation with temperature (Cahyarini et al., 2009). Unlike the results reported by de Villiers et al. (1994), that study finds that the horizontal core had lower coral Sr/Ca values (i.e., higher temperature) with lower extension rates (9.7 mm year^{-1}) suggesting something else is altering coral Sr/Ca other than growth-related effects or changes in temperature with water depth. These differences may be related to thermal stress as the top of the colony reaches the water surface leading to a breakdown of the coral Sr/Ca thermometer (Marshall and McCulloch, 2002; Liu et al., 2005; Felis et al., 2009). Conversely, *Porites* microatolls, colonies in very shallow water that no longer extend vertically but laterally, have approximately the same mean coral $\delta^{18}O$ values between transects and good correlation with temperature suggesting microatolls are more thermally tolerant than a boulder-shaped *Porites* colony growing towards the surface (McGregor et al., 2011).

We find growth-related effects are not influencing our optimally sampled coral Sr/Ca variations. Our results for coral Sr/Ca generally agree with the extension rate limit of 6.0 mm year^{-1} set by Felis et al. (2003) determined from $\delta^{18}O$ determinations in *Porites* spp. Furthermore, we find coral Sr/Ca determinations are reproducible for extension rates between 5 and 6 mm year^{-1} compared with optimally sampled determinations with extension rates >7 mm year^{-1}. A study that examined a *Pavona clavus* colony suggests 5 mm year^{-1} as the minimum extension rate for growth-related effects (McConnaughey, 1989). Conversely, the slow growing and more dense massive corals *Diploastrea heliopora* and *Siderastrea siderea* have average extension rates of ~5.5 and ~4.5 mm year^{-1}, respectively, and replication studies with these corals reveal reproducible coral Sr/Ca determinations within and between colonies (Bagnato et al., 2004; DeLong et al., 2011). These results suggest the growth-related effects vary with species and calcification rate, not extension rate, thus calcification is more important in determining thresholds for kinetic effects.

The initial studies reporting differences between horizontal and vertical samples examined a columnar coral, *Pavona clavus*, in which growth rates vary greatly (~200%) between the sides and the vertical top of the colony (McConnaughey, 1989; de Villiers et al., 1994, 1995) whereas the differences in growth rates along the surface of a massive

Porites colony are not large, ~15% (Lough and Barnes, 2000). Branching corals are the extreme in regards to extension rates; these corals have fast growing axial corallites (~100 mm year^{-1}) and slow growing radial corallites (<10 mm year^{-1}). Coral Sr/Ca and δ^{18}O determinations from the branching coral *Acropora noblis* are significantly different between the radial and axial corallites with no significant correlation with temperature (Shirai et al., 2008). Conversely, a culture experiment with a branching species of *Porites* finds that the coral Sr/Ca to temperature slope is within the range of slopes determined for massive *Porites* spp. (Armid et al., 2011). These results suggest that the same process for the incorporation of strontium in coral skeletal material for branching forms of *Porites* is similar to that of massive forms of this species. On the other end of the growth rate scale, no significant differences are present between synchronous horizontal and vertical paths in the slow growing (4.5 mm year^{-1}) massive coral *Siderastrea siderea* (DeLong et al., 2012b). The relationship, if there is one, between colony morphology, species, growth rate, and geochemistry is unclear; nevertheless, it is apparent that broad generalizations cannot be made with regards to kinetic effects.

5.3. Chronology error

Combining cross dating and high precision ^{230}Th dating (Shen et al., 2008) allows us to determine an absolute chronology and to evaluate chronology error for reconstructions based on a single core. We compare our chronology with a previous study (Quinn et al., 1998) based the single core 92-PAA1, which is included in this study (Fig. 9 and Table 6). The previous study established their chronology by assuming a minimal loss of time between breaks in the core. They selected continuous paths (green paths in Fig. 1) except when a path ends or when density bands are not apparent in the X-radiographs and then they selected new paths that overlap in time, if possible (e.g., 92-PAA1-B and 92-PAA1-N in Fig. 1). Cross dating reveals the core section 92-PAA1-I is synchronous with the top of 92-PAA1-H (1732 to 1729 CE; Fig. 1) because the coral grew around the cavity resulting in false years in the previous study's chronology thus a 9-year difference between the chronologies. The previous study had a core bottom date of 1657 CE for 92-PAA1 (Quinn et al., 1998); however, we interpret the last 2 years as false years caused by suboptimal corallite alignment (Fig. 1 and Table 2). We test the assumption of minimal time loss and we find little missing time for core sections with continuous paths yet core breaks without continuous paths and core sections with disorganized corallites result in missing years (total of 4.5 years; Table 6) and false years (total of 12.5 years). Combination of missing and false years reduces the overall chronology error to −2.3 years century^{-1} for which the chronology error increases with age or down core (Fig. 9).

We perform a hypothetical experiment with the core 92-PAA2 in which we make the same assumptions as the study of Quinn et al. (1998) and we determine the chronology for a single core (Table 6). The time missing between the core sections in 92-PAA2 is relatively small, <8 months, until 1722 CE (J→K in Table 6). The largest contributor to chronology error in the core 92-PAA2 is the gap between core sections 92-PAA2-K and 92-PAA2-L (1699 to 1708 CE), which results in 9.25 years missing, whereas the largest contributor in the core 92-PAA1 is false years. The core bottom date for 92-PAA2 is 1662 CE for a chronology based on just that core, 13 years younger than cross-dated bottom date, yielding a chronology error of +3.7 years century^{-1}.

Overall, the assumption of minimal time loss between core sections is correct when density bands are clear in the X-radiographs and a minimal loss of material occurs during core recovery. This assumption does not hold true when the density band structure becomes less clear down core and when the centimeter-scale growth structures meander producing fewer optimal paths to sample. The chronology uncertainty increases in both of our cores ~2.8 m or ~250 years down the core. A survey of X-radiographs from other multi-century studies with massive *Porites* colonies reveals that corallite fans tend to meander ~250 years down the core (e.g., Linsley et al., 1994; Felis et al., 2000; Ren et al., 2002; Linsley et al., 2004; Zinke et al., 2004; Linsley et al., 2008). One study finds increased dating uncertainties caused by centimeter-scale skeletal structures at only 40 years down core (Alibert and Kinsley, 2008). This difference may reflect the fact that researchers pick the best cores for their reconstructions. Chronology error depends on the quality of the core and the growth structures in the core. A core with many breaks or disorganized corallites will have larger annual chronology error than a core with clear density bands and few breaks. For example, 92-PAA2 has few breaks, clear density bands, and optimal corallite fans until 1709 CE when disorganized corallites perturb the record. Improvements to core drilling may aid in recovery of cores from large *Porites* colonies yet meandering corallite fans may still be present. The study by Lough and Barnes (1992) examined forty colonies from the Great Barrier Reef and they report, "…it was impossible to cut a slice from a single growth axis in such large colonies of *Porites*."

Our chronology error assessment for reconstructions composed of a single core (−2.3 to +3.7 years century^{-1}) is within previous estimates of ±1 to 5 years century^{-1} (Swart et al., 1996b; Dunbar and Cole, 1999; Felis et al., 2000; DeLong et al., 2007; Shen et al., 2008). These estimates are concerning for reconstructions of interannual climate variability such as El Niño–Southern Oscillation and decadal scale variability. A reconstruction of 300 years could possibly have a shift of 9 years in the last century of the record thus changing interpretation of the duration and timing of climatic events. Furthermore, chronological error can influence the frequency domain interpretation of high-resolution reconstructions (DeLong et al., 2009).

6. Conclusions

Producing multi-century geochemical records from corals is time consuming and expensive, yet these reconstructions are invaluable contributions to our understanding of tropical climate variability. Unfortunately, these long records are few and each core recovered from a coral colony is invaluable. In lieu of replication with many colonies, some paleoclimatologists have used the multi-proxy approach to replicate and isolate climatic signals contained in corals. This study started as a multi-proxy study to complement to the coral δ^{18}O study of Quinn et al. (1998); however, we found discrepancies that we could not explain at first. We consulted with dendroclimatologists who suggested that the answers might be revealed by re-examining methods and by going back to "the wood" or in our case, the coral. Sampling a coral for a paleoclimate reconstruction is simple, follow the coral's growth through time; however, this growth axis is not always readily apparent. Some studies focus on biomineralization and micro-scale structures in order to understand how corals form their skeleton in relation to the incorporation of trace elements and heavier isotopes. A few studies focus on centimeter-scale structures and their relationship to growth and the inclusive records. Our study went back to the coral, the coral slab, and the growth structures visible on the slab surface. X-radiographs are helpful in identifying sampling paths but they can be misleading and they are no substitute for looking at the coral. We find sampling along the axis of major growth on the corallite fans with corallites parallel to the surface yields reproducible geochemical time series within and between colonies, as long as extension rates are above the threshold for that species. We find that coral Sr/Ca determinations are more sensitive to sampling path selection than coral δ^{18}O determinations. Strontium is a trace element in coral calcium carbonate whereas oxygen is a major constituent and is thus less sensitive to sample path selection.

The results presented here demonstrate that coral Sr/Ca variations from multi-century long intracolony cores can yield highly reproducible records that can be cross-dated to reduce chronology error and can be used to produce a temperature reconstruction with high fidelity. Our optimal sampling method will allow paleoclimatologists to recover Sr/Ca, δ^{18}O, as well as other records from corals with greater

accuracy and precision. Re-examination of previous coral-based studies, similar to ours, can be carried out with little cost by examining core slabs and the geochemical records from those slabs. Resampling intervals with disorganized or suboptimal corallites may resolve discrepancies between records and provide new insight into past climate variability. Furthermore, our optimal sampling method will be useful for corals without clear annual density bands, if the corallite fans are present on the slab surface. The results from our horizontal and vertical comparison give promise for both modern and subfossil coral reconstructions. Some researchers may have disregarded cores that did not have prefect vertical transects or cores for which the orientation with respect to the colony is unknown. We suggest that these cores from massive *Porites* colonies can be used, as long as extension rates are above the threshold for this coral genus, no indications of diagenesis or thermal stress are present, and our optimal sampling method is used. We cannot make the same conclusions for other coral genera and we suggest caution in making broad generalizations between coral genera and different coral morphologies. Our hope is that this research will further the use of Sr/Ca variations in corals to reconstruct tropical ocean temperatures in order to address important questions regarding our changing world.

7. Recommendations

1. Selection of sampling paths for geochemical and growth studies needs to include the additional step of examining the coral slab to locate corallite fans with a central axis along the slab surface in which the rods and rungs of the corallites are parallel to the slab surface. Our optimal sampling method ensures that sampling paths follow the time axis of the coral colony.
2. We find that corallite alignment to the slab surface is more important than sampling directly on central apex of the corallite fan; however, paths off the apex should be avoided if possible.
3. We suggest monitoring extension rates for indications of suboptimal and disorganized corallites as well as growth-related effects. This monitoring can be carried out using X-radiographs for new studies and by examining the distance between geochemical maxima for previous studies. Extension rates should be relatively smooth without anomalously short or long years, which may indicate that sampling paths are not parallel to the growth axis of the corallite fan. For *Porites* spp., the minimum extension rate is between 5 and 6 mm year^{-1}.
4. We recommend sampling two cores from the same colony and cross dating the records for reconstructions longer than 250 years. This is necessary to reduce chronology error and to recover a complete record as well as reduce non-environmental variability. High-precision ^{230}Th dating will aid in cross dating cores and allow researchers to verify their chronologies.
5. X-radiographs should be included in reports of coral studies in order to evaluate sample path selection. Any areas with suboptimal or problematic corallite alignment should be noted and avoided. We find using high-resolution digital X-radiography is able to resolve density bands in corals previously thought to not contain density bands; therefore, re-examination of coral slabs from earlier studies may be beneficial.

Acknowledgments

Financial support provided by the Gulf Oceanographic Charitable Trust and the Carl Riggs Endowed Fellowships of the University of South Florida, College of Marine Science, Louisiana State University Summer Research Award, and the National Science Foundation is gratefully acknowledged. U–Th isotopic determinations and ^{230}Th age calculation were supported by ROC NSC grants (NSC 99-2628-M-002-012 and 100-2116-M-002-009) to C.-C.S. We thank Christy Stephans for providing coral data and Thierry Corrége, Timothée Ourbak, and IRD-ECOP for providing temperature data. We thank Ethan Goddard, Chris Maupin, Liz Dunn, Kelly Herid, and Meaghan Gorman for analytical assistance; Tony Greco, Hali Kilbourne, and Noreen Buster for assistance with SEM images, thin section photomicrographs, and X-radiographs, respectively. Finally, we thank Malclom Hughes, Ramzi Touchan, and The Laboratory of Tree-Ring Research at the University of Arizona for providing summer workshops, for sharing their knowledge and sage advice. The data is available from the IGBP PAGES/World Data Center for Paleoclimatology, http://www.ncdc.noaa.gov/paleo/paleo.html, Data Contribution Series # 2012-085.

Appendix A. Supplementary data

Supplementary data associated with this article can be found in the online version, at http://dx.doi.org/10.1016/j.palaeo.2012.08.019. These data include Google maps of the most important areas described in this article.

References

Alibert, C., Kinsley, L., 2008. A 170-year Sr/Ca and Ba/Ca coral record from the western Pacific warm pool: 1. What can we learn from an unusual coral record? Journal of Geophysical Research 113, C04008 http://dx.doi.org/10.1029/2006JC003979.

Alibert, C., McCulloch, M.T., 1997. Strontium/calcium ratios in modern *Porites* corals from the Great Barrier Reef as a proxy for sea surface temperature: Calibration of the thermometer and monitoring of ENSO. Paleoceanography 12, 345–363 http://dx.doi.org/10.1029/97PA00318.

Armid, A., Asami, R., Fahmiati, T., Sheikh, M.A., Fujimura, H., Higuchi, T., Taira, E., Shinjo, R., Oomori, T., 2011. Seawater temperature proxies based on D_{Sr}, D_{Mg}, and D_U from culture experiments using the branching coral *Porites cylindrica*. Geochimica et Cosmochimica Acta 75, 4273–4285 http://dx.doi.org/10.1016/j.gca.2011.05.010.

Bagnato, S., Linsley, B.K., Howe, S.S., Wellington, G.M., Salinger, J., 2004. Evaluating the use of the massive coral *Diploastrea heliopora* for paleoclimate reconstruction. Paleoceanography 19, PA1032 http://dx.doi.org/10.1029/2003PA000935.

Barnes, D.J., 1973. Growth in colonial Scleractinians. Bulletin of Marine Science 23, 280–298.

Barnes, D.J., Lough, J.M., 1989. The nature of skeletal density banding in scleractinian corals: fine banding and seasonal patterns. Journal of Experimental Marine Biology and Ecology 126, 119–134.

Barnes, D.J., Lough, J.M., 1993. On the nature and causes of density banding in massive coral skeletons. Journal of Experimental Marine Biology and Ecology 167, 91–108 http://dx.doi.org/10.1016/0022-0981(93)90186-R.

Barnes, D.J., Lough, J.M., Tobin, B.J., 1989. Density measurements and the interpretation of X-radiographic images of slices of skeleton from the colonial hard coral *Porites*. Journal of Experimental Marine Biology and Ecology 131, 45–60 http://dx.doi.org/10.1016/0022-0981(89)90010-5.

Barnes, D.J., Taylor, R.B., Lough, J.M., 1995. On the inclusion of trace materials into massive coral skeletons. Part II: distortions in skeletal records of annual climate cycles due to growth processes. Journal of Experimental Marine Biology and Ecology 194, 251–275 http://dx.doi.org/10.1016/0022-0981(95)00091-7.

Bloomfield, P., 2000. Fourier Analysis of Time Series: An Introduction, Second ed. John Wiley & Sons, New York.

Brown, D., Basch, L., Barshis, D., Forsman, Z., Fenner, D., Goldberg, J., 2009. American Samoa's island of giants: Massive *Porites* colonies at Ta'u island. Coral Reefs 28, 735-735 http://dx.doi.org/10.1007/s00338-009-0494-8.

Cahyarini, S.Y., Pfeiffer, M., Dullo, W.C., 2009. Improving SST reconstructions from coral Sr/Ca records: multiple corals from Tahiti (French Polynesia). International Journal of Earth Sciences 98, 31–40 http://dx.doi.org/10.1007/s00531-008-0323-2.

Calvo, E., Marshall, J.F., Pelejero, C., McCulloch, M.T., Gagan, M.K., Lough, J.M., 2007. Interdecadal climate variability in the Coral Sea since 1708 A.D. Palaeogeography, Palaeoclimatology, Palaeoecology 248, 190–201 http://dx.doi.org/10.1016/j.palaeo.2006.12.003.

Cheng, H., Edwards, R.L., Hoff, J., Gallup, C.D., Richards, D.A., Asmerom, Y., 2000. The half-lives of uranium-234 and thorium-230. Chemical Geology 169, 17–33 http://dx.doi.org/10.1016/S0009-2541(99)00157-6.

Cohen, A.L., Hart, S.R., 1997. The effect of colony topography on climate signals in coral skeleton. Geochimica et Cosmochimica Acta 61, 3905.

Cohen, A.L., Smith, S.R., McCartney, M.S., van Etten, J., 2004. How brain corals record climate: an integration of skeletal structure, growth and chemistry of *Diploria labyrinthiformis* from Bermuda. Marine Ecology Progress Series 271, 147–158.

Corrège, T., 2006. Sea surface temperature and salinity reconstruction from coral geochemical tracers. Palaeogeography, Palaeoclimatology, Palaeoecology 232, 408–428 http://dx.doi.org/10.1016/j.palaeo.2005.10.014.

Corrège, T., Quinn, T., Delcroix, T., Le Cornec, F., Recy, J., Cabioch, G., 2001. Little Ice Age sea surface temperature variability in the southwest tropical Pacific. Geophysical Research Letters 28, 3477–3480 http://dx.doi.org/10.1029/2001GL013216.

Crowley, T.J., Quinn, T.M., Hyde, W.T., 1999. Validation of coral temperature calibrations. Paleoceanography 14, 605–615 http://dx.doi.org/10.1029/1999PA900032.

Darke, W.M., Barnes, D.J., 1993. Growth trajectories of corallites and ages of polyps in massive colonies of reef-building corals of the genus *Porites*. Marine Biology 117, 321–326 http://dx.doi.org/10.1007/BF00345677.

de Villiers, S., Shen, G.T., Nelson, B.K., 1994. The Sr/Ca-temperature relationship in coralline aragonite: influence of variability in $(Sr/Ca)_{seawater}$ and skeletal growth parameters. Geochimica et Cosmochimica Acta 58, 197–208 http://dx.doi.org/10.1016/0016-7037(94)90457-x.

de Villiers, S., Nelson, B.K., Chivas, A.R., 1995. Biological controls on coral Sr/Ca and $\delta^{18}O$ reconstructions of sea surface temperatures. Science 269, 1247–1249 http://dx.doi.org/10.1126/science.269.5228.1247.

DeLong, K.L., Quinn, T.M., Taylor, F.W., 2007. Reconstructing twentieth-century sea surface temperature variability in the southwest Pacific: a replication study using multiple coral Sr/Ca records from New Caledonia. Paleoceanography 22, PA4212 http://dx.doi.org/10.1029/2007PA001444.

DeLong, K.L., Quinn, T.M., Mitchum, G.T., Poore, R.Z., 2009. Evaluating highly resolved paleoclimate records in the frequency domain for multidecadal-scale climate variability. Geophysical Research Letters 36, L20702 http://dx.doi.org/10.1029/2009gl039742.

DeLong, K.L., Quinn, T.M., Shen, C.-C., Lin, K., 2010. A snapshot of climate variability at Tahiti 9.5 ka using a fossil coral from IODP expedition 310. Geochemistry, Geophysics, Geosystems 11, Q06005 http://dx.doi.org/10.1029/2009GC002758.

DeLong, K.L., Flannery, J.A., Maupin, C.R., Poore, R.Z., Quinn, T.M., 2011. A coral Sr/Ca calibration and replication study of two massive corals from the Gulf of Mexico. Palaeogeography, Palaeoclimatology, Palaeoecology 307, 117–128 http://dx.doi.org/10.1016/j.palaeo.2011.05.005.

DeLong, K.L., Quinn, T.M., Taylor, F.W., Lin, K., Shen, C.-C., 2012a. Sea surface temperature variability in the southwest tropical Pacific since AD 1649. Nature Climate Change http://dx.doi.org/10.1038/nclimate1583.

DeLong, K.L., Maupin, C.R., Flannery, J.A., Quinn, T.M., Shen, C.-C., Lin, K., 2012b. Decadal variability in Gulf of Mexico sea surface temperatures since 1734 CE. American Geophysical Union Fall Meeting, San Francisco, CA, pp. Fall Meet. Suppl., Control id: 1485115.

DeLong, K.L., Quinn, T.M., Taylor, F.W., Shen, C.-C., Lin, K., in revision. Non-environmental variability in massive corals assessed by replicating geochemical signals in massive corals. Palaeogeography, Palaeoclimatology, Palaeoecology.

Draper, N.R., Smith, H., 1998. Applied Regression Analysis, Third ed. Wiley-Interscience Publication, New York.

Dunbar, R.B., Cole, J.E., 1992. Coral records of ocean-atmosphere variability. Workshop on Coral Paleoclimate Reconstruction. NOAA, La Parguera, Puerto Rico.

Dunbar, R.B., Cole, J.E., 1999. Annual Records of Tropical Systems (ARTS): Recommendations for Research. PAGES/CLIVAR, Kauai, Hawaii.

Fairbanks, R.G., Dodge, R.E., 1979. Annual periodicity of the $^{18}O/^{16}O$ and $^{13}C/^{12}C$ ratios in the coral *Montastrea annularis*. Geochimica et Cosmochimica Acta 43, 1009–1020 http://dx.doi.org/10-1017/s00338-003-03225.

Felis, T., Pätzold, J., Loya, Y., Fine, M., Nawar, A.H., Wefer, G., 2000. A coral oxygen isotope record from the northern Red Sea documenting NAO, ENSO, and North Pacific teleconnections on Middle East climate variability since the year 1750. Paleoceanography 15, 679–694 http://dx.doi.org/10.1029/1999PA000477.

Felis, T., Pätzold, J., Loya, Y., 2003. Mean oxygen-isotope signatures in *Porites* spp. corals: inter-colony variability and correction for extension-rate effects. Coral Reefs 22, 328–336 http://dx.doi.org/10.1007/s00338-003-0324-3.

Felis, T., Suzuki, A., Kuhnert, H., Dima, M., Lohmann, G., Kawahata, H., 2009. Subtropical coral reveals abrupt early-twentieth-century freshening in the western North Pacific Ocean. Geology 37, 527–530 http://dx.doi.org/10.1130/g25581a.1.

Fritts, H.C., 1976. Tree Rings and Climate. The Blackburn Press, Caldwell, NJ.

Frohlich, C., Hornbach, M.J., Taylor, F.W., Shen, C.-C., Moala, A., Morton, A.E., Kruger, J., 2009. Huge erratic boulders in Tonga deposited by a prehistoric tsunami. Geology 37, 131–134 http://dx.doi.org/10.1130/G25277A.1.

Gagan, M.K., Dunbar, G.B., Suzuki, A., 2012. The effect of skeletal mass accumulation in *Porites* on coral Sr/Ca and $\delta^{18}O$ paleothermometry. Paleoceanography 27, PA1203 http://dx.doi.org/10.1029/2011pa002215.

Giry, C., Felis, T., Kölling, M., Scheffers, S., 2010. Geochemistry and skeletal structure of *Diploria strigosa*, implications for coral-based climate reconstruction. Palaeogeography, Palaeoclimatology, Palaeoecology 298, 378–387 http://dx.doi.org/10.1016/j.palaeo.2010.10.022.

Grootes, P.M., Stuiver, M., White, J.W.C., Johnsen, S., Jouzel, J., 1993. Comparison of oxygen isotope records from the GISP2 and GRIP Greenland ice cores. Nature 366, 552–554.

Heiss, G.A., Dullo, W.-C., Joachimski, M.M., Reijmer, J.J.G., Schuhmacher, H., 1999. Increased seasonality in the Gulf of Aqaba, Red Sea, recorded in the oxygen isotope record of a *Porites lutea* coral. Senckenbergiana Maritima 30, 17–26.

Hendy, E.J., Gagan, M.K., Alibert, C.A., McCulloch, M.T., Lough, J.M., Isdale, P.J., 2002. Abrupt decrease in tropical Pacific sea surface salinity at end of Little Ice Age. Science 295, 1511–1514 http://dx.doi.org/10.1126/science.1067693.

Hendy, E.J., Gagan, M.K., Lough, J.M., 2003. Chronological control of coral records using luminescent lines and evidence for non-stationary ENSO teleconnections in northeast Australia. The Holocene 13, 187–199 http://dx.doi.org/10.1191/0959683603hl606rp.

Hendy, E., Gagan, M.K., Lough, J.M., McCulloch, M., deMenocal, P.B., 2007. Impact of skeletal dissolution and secondary aragonite on trace element and isotopic climate proxies in *Porites* corals. Paleoceanography 22, PA4101 http://dx.doi.org/10.1029/2007PA001462.

Hudson, J.H., Shinn, E.A., Halley, R.B., Lidz, B., 1976. Sclerochronology: a tool for interpreting past environments. Geology 4, 361–364.

Jaffey, A.H., Flynn, K.F., Glendenin, L.E., Bentley, W.C., Essling, A.M., 1971. Precision measurement of half-lives and specific activities of ^{235}U and ^{238}U. Physical Review C 4, 1889–1906 http://dx.doi.org/10.1103/PhysRevC.4.1889.

Jones, P.D., Briffa, K.R., Osborn, T.J., Lough, J.M., van Ommen, T.D., Vinther, B.M., Luterbacher, J., Wahl, E.R., Zwiers, F.W., Mann, M.E., Schmidt, G.A., Ammann, C.M., Buckley, B.M., Cobb, K.M., Esper, J., Goosse, H., Graham, N., Jansen, E., Kiefer, T., Kull, C., Kuttel, M., Mosley-Thompson, E., Overpeck, J.T., Riedwyl, N., Schulz, M., Tudhope, A.W., Villalba, R., Wanner, H., Wolff, E., Xoplaki, E., 2009. High-resolution palaeoclimatology of the last millennium: a review of current status and future prospects. The Holocene 19, 3–49 http://dx.doi.org/10.1177/0959683608098952.

Knutson, D., Buddemeier, R., Smith, S., 1972. Coral chronometers: seasonal growth bands in reef corals. Science 177, 270–272 http://dx.doi.org/10.1126/science/177.4045.270.

Kuhnert, H., Pätzold, J., Schnetger, B., Wefer, G., 2002. Sea-surface temperature variability in the 16th century at Bermuda inferred from coral records. Palaeogeography, Palaeoclimatology, Palaeoecology 179, 159–171.

Land, L.S., Lang, J.C., Barnes, D.J., 1975. Extension rate: a primary control on the isotopic composition of West Indian (Jamaican) scleractinian reef coral skeletons. Marine Biology 33, 221–233.

Leder, J.J., Swart, P.K., Szmant, A.M., Dodge, R.E., 1996. The origin of variations in the isotopic record of scleractinian corals: I. Oxygen. Geochimica et Cosmochimica Acta 60, 2857–2870.

Linsley, B.K., Dunbar, R.B., Wellington, G.M., Mucciarone, D.A., 1994. A coral-based reconstruction of intertropical convergence zone variability over Central America since 1707. Journal of Geophysical Research 99 (C5), 9977–9994 http://dx.doi.org/10.1029/94JC00360.

Linsley, B.K., Wellington, G.M., Schrag, D.P., 2000. Decadal sea surface temperature variability in the subtropical South Pacific from 1726 to 1997 AD. Science 290, 1145–1148 http://dx.doi.org/10.1126/science.290.5494.1145.

Linsley, B.K., Wellington, G.M., Schrag, D.P., Ren, L., Salinger, M.J., Tudhope, A.W., 2004. Geochemical evidence from corals for changes in the amplitude and spatial pattern of South Pacific interdecadal climate variability over the last 300 years. Climate Dynamics 22, 1–11 http://dx.doi.org/10.1007/s00382-003-0364-y.

Linsley, B.K., Kaplan, A., Gouriou, Y., Salinger, J., deMenocal, P.B., Wellington, G.M., Howe, S.S., 2006. Tracking the extent of the South Pacific convergence zone since the early 1600s. Geochemistry, Geophysics, Geosystems 7, Q05003 http://dx.doi.org/10.1029/2005GC001115.

Linsley, B.K., Zhang, P., Kaplan, A., Howe, S.S., Wellington, G.M., 2008. Interdecadal-decadal climate variability from multi-coral oxygen isotope records in the South Pacific convergence zone region since 1650 A.D. Paleoceanography 23, PA2219 http://dx.doi.org/10.1029/2007PA001539.

Liu, J., Crowley, T.J., Quinn, T.M., 2005. Breakdown of Sr/Ca paleothermometer in a coral record from New Georgia, West Pacific warm pool. Fall Meet. Suppl., Abstract PP44A-07: Eos Trans. AGU, 86.

Lough, J.M., 2004. A strategy to improve the contribution of coral data to high-resolution paleoclimatology. Palaeogeography, Palaeoclimatology, Palaeoecology 204, 115–143 http://dx.doi.org/10.1016/S0031-0182(03)00727-2.

Lough, J.M., Barnes, D.J., 1990. Intra-annual timing of density band formation of *Porites* coral from the central Great Barrier Reef. Journal of Experimental Marine Biology and Ecology 135, 35–57 http://dx.doi.org/10.1016/0022-098(90)90197-R.

Lough, J.M., Barnes, D.J., 1992. Comparisons of skeletal density variations in *Porites* from the central Great Barrier Reef. Journal of Experimental Marine Biology and Ecology 155, 1–25 http://dx.doi.org/10.1016/0022-0981(92)90024-5.

Lough, J.M., Barnes, D.J., 1997. Several centuries of variation in skeletal extension, density and calcification in massive *Porites* colonies from the Great Barrier Reef: a proxy for seawater temperature and a background of variability against which to identify unnatural change. Journal of Experimental Marine Biology and Ecology 211, 29–67 http://dx.doi.org/10.1016/50022-0981(96)02710-4.

Lough, J.M., Barnes, D.J., 2000. Environmental controls on growth of the massive coral *Porites*. Journal of Experimental Marine Biology and Ecology 245, 225–243.

Lough, J.M., Cooper, T.F., 2011. New insights from coral growth band studies in an era of rapid environmental change. Earth-Science Reviews 108, 170–184 http://dx.doi.org/10.1016/j.earscirev.2011.07.001.

Maier, C., Felis, T., Patzold, J., Bak, R.P.M., 2004. Effect of skeletal growth and lack of species effects in the skeletal oxygen isotope climate signal within the coral genus *Porites*. Marine Geology 207, 193–208 http://dx.doi.org/10.1016/j.margeo.2004.03.008.

Marshall, J.F., McCulloch, M.T., 2002. An assessment of the Sr/Ca ratio in shallow water hermatypic corals as a proxy for sea surface temperature. Geochimica et Cosmochimica Acta 66, 3263–3280 http://dx.doi.org/10.1016/5016-7037(20)00926-2.

McConnaughey, T., 1989. ^{13}C and ^{18}O isotopic disequilibrium in biological carbonates: I. Patterns. Geochimica et Cosmochimica Acta 53, 151–162 http://dx.doi.org/10.1016/0016-7037(89)90282-2.

McGregor, H.V., Gagan, M.K., 2003. Diagenesis and geochemistry of *Porites* corals from Papua New Guinea: implications for paleoclimate reconstruction. Geochimica et Cosmochimica Acta 67, 2147–2156.

McGregor, H.V., Fischer, M.J., Gagan, M.K., Fink, D., Woodroffe, C.D., 2011. Environmental control of the oxygen isotope composition of *Porites* coral microatolls. Geochimica et Cosmochimica Acta 75, 3930–3944 http://dx.doi.org/10.1016/j.gca.2011.04.017.

Mitsuguchi, T., Matsumoto, E., Uchida, T., 2003. Mg/Ca and Sr/Ca ratios of *Porites* coral skeleton: evaluation of the effect of skeletal growth rate. Coral Reefs 22, 381–388 http://dx.doi.org/10.1007/S00338-003-0326-1.

Ourbak, T., DeLong, K.L., Corrège, T., Malaizé, B., Kilbourne, K.H., Caquineau, S., Hollander, D.J., 2008. The significance of geochemical proxies in corals, does size (age) matter? International Coral Reef Symposium. Proceedings of the 11th International Coral Reef Symposium, Ft. Lauderdale, Florida, pp. 82–86.

Paillard, D., Labeyrie, L., Yiou, P., 1996. Macintosh program performs time-series analysis. Eos Trans. AGU, 77, p. 379.

Peterson, L.C., Haug, G.H., Murray, R.W., Yarincik, K.M., King, J.W., Bralower, T.J., Kameo, K., Rutherford, S.D., Pearce, R.B., 2000. Late Quaternary stratigraphy and sedimentation at site 1002, Cariaco Basin (Venezuela). Proceedings of the Ocean Drilling Program: Scientific Results, 165, pp. 85–99.

Quinn, T.M., Sampson, D.E., 2002. A multiproxy approach to reconstructing sea surface conditions using coral skeleton geochemistry. Paleoceanography 17, 1062 http://dx.doi.org/10.1029/2000PA000528.

Quinn, T.M., Taylor, F.W., 2006. SST artifacts in coral proxy records produced by early marine diagenesis in a modern coral from Rabaul, Papua New Guinea. Geophysical Research Letters 33, L04601 http://dx.doi.org/10.1029/2005GL024972.

Quinn, T.M., Taylor, F.W., Crowley, T.J., Link, S.M., 1996. Evaluation of sampling resolution in coral stable isotope records: a case study using records from New Caledonia and Tarawa. Paleoceanography 11, 529–542 http://dx.doi.org/10.1029/96PA01859.

Quinn, T.M., Crowley, T.J., Taylor, F.W., Henin, C., Joannot, P., Join, Y., 1998. A multicentury stable isotope record from a New Caledonia coral: interannual and decadal sea surface temperature variability in the southwest Pacific since 1657 A.D. Paleoceanography 13, 412–426 http://dx.doi.org/10.1029/98PA00401.

Rayner, N.A., Parker, D.E., Horton, E.B., Folland, C.K., Alexander, L.V., Rowell, D.P., Kent, E.C., Kaplan, A., 2003. Global analyses of SST, sea ice, and night marine air temperature since the late nineteenth century. Journal of Geophysical Research 108, 4407 http://dx.doi.org/10.1029/2002JD002670.

Ren, L., Linsley, B.K., Wellington, G.M., Schrag, D.P., Hoegh-Guldberg, O., 2002. Deconvolving the δ^{18}O seawater component from subseasonal coral δ^{18}O and Sr/Ca at Rarotonga in the southwestern subtropical Pacific for the period 1726 to 1997. Geochimica et Cosmochimica Acta 67, 1609–1621 http://dx.doi.org/10.1016/50016-7037(2)00917-1.

Scott, R.B., Holland, C.L., Quinn, T.M., 2010. Multidecadal trends in instrumental SST and coral proxy Sr/Ca records. Journal of Climate 1017–1033 http://dx.doi.org/10.1175/2009JCLI2386.1.

Shen, C.-C., Lee, T., Chen, C.-Y., Wang, C.-H., Dai, C.-F., Li, L.-A., 1996. The calibration of *D*[Sr/Ca] versus sea surface temperature relationship for *Porites* corals. Geochimica et Cosmochimica Acta 60, 3849–3858 http://dx.doi.org/10.1016/0016-7037(96)00205-0.

Shen, C.-C., Lawrence Edwards, R., Cheng, H., Dorale, J.A., Thomas, R.B., Bradley Moran, S., Weinstein, S.E., Edmonds, H.N., 2002. Uranium and thorium isotopic and concentration measurements by magnetic sector inductively coupled plasma mass spectrometry. Chemical Geology 185, 165–178 http://dx.doi.org/10.1016/s0009-2541(01)00404-1.

Shen, C.-C., Cheng, H., Edwards, R.L., Moran, S.B., Edmonds, H.N., Hoff, J.A., Thomas, R.B., 2003. Measurement of attogram quantities of ^{231}Pa in dissolved and particulate fractions of seawater by isotope dilution thermal ionization mass spectroscopy. Analytical Chemistry 75, 1075–1079 http://dx.doi.org/10.1021/ac026247r.

Shen, C.-C., Li, K.-S., Sieh, K., Natawidjaja, D., Cheng, H., Wang, X., Edwards, R.L., Lam, D.D., Hsieh, Y.-T., Fan, T.-Y., Meltzner, A.J., Taylor, F.W., Quinn, T.M., Chiang, H.-W., Kilbourne, K.H., 2008. Variation of initial ^{230}Th/^{232}Th and limits of high precision U–Th dating of shallow-water corals. Geochimica et Cosmochimica Acta 72, 4201–4223 http://dx.doi.org/10.1016/j.gca.2008.06.011.

Shen, C.-C., Kano, A., Hori, M., Lin, K., Chiu, T.-C., Burr, G.S., 2010. East Asian monsoon evolution and reconciliation of climate records from Japan and Greenland during the last deglaciation. Quaternary Science Reviews 29, 3327–3335 http://dx.doi.org/10.1016/j.quascirev.2010.08.012.

Shirai, K., Kawashima, T., Sowa, K., Watanabe, T., Nakamori, T., Takahata, N., Amakawa, H., Sano, Y., 2008. Minor and trace element incorporation into branching coral *Acropora nobilis* skeleton. Geochimica et Cosmochimica Acta 72, 5386–5400 http://dx.doi.org/10.1016/j.gca.2008.07.026.

Smith, J.M., Quinn, T.M., Helmle, K.P., Halley, R.B., 2006. Reproducibility of geochemical and climatic signals in the Atlantic coral *Montastraea faveolata*. Paleoceanography 21, PA1010 http://dx.doi.org/10.1029/2005PA001187.

Stephans, C., Quinn, T.M., Taylor, F.W., Corrège, T., 2004. Assessing the reproducibility of coral-based climate records. Geophysical Research Letters 31, L18210 http://dx.doi.org/10.1029/2004GL020343.

Swart, P.K., Dodge, R.E., Hudson, H.J., 1996a. A 240-year stable oxygen and carbon isotopic record in a coral from South Florida: implications for the prediction of precipitation in southern Florida. Palaios 11, 362–375.

Swart, P.K., Healy, G.F., Dodge, R.E., Kramer, P., Hudson, J.H., Halley, R.B., Robblee, M.B., 1996b. The stable oxygen and carbon isotopic record from a coral growing in Florida Bay: a 160 year record of climatic and anthropogenic influence. Palaeogeography, Palaeoclimatology, Palaeoecology 123, 219–237.

Urban, F.E., Cole, J.E., Overpeck, J.T., 2000. Influence of mean climate change on climate variability from a 155-year tropical Pacific coral record. Nature 407, 989–993.

Veron, J.E.N., 1986. Corals of Australia and the Indo-Pacific. Univeristy of Hawaii Press, North Ryde, NSW, Australia . edition ed. Univeristy of Hawaii Press edition.

Watanabe, T., Gagan, M.K., Corrège, T., Scott-Gagan, H., Cowley, J., Hantoro, W.S., 2003. Oxygen isotope systematics in *Diploastrea heliopora*: new coral archive of tropical paleoclimate. Geochimica et Cosmochimica Acta 67, 1349–1358.

Zinke, J., Dullo, W.C., Heiss, G.A., Eisenhauer, A., 2004. ENSO and Indian Ocean subtropical dipole variability is recorded in a coral record off southwest Madagascar for the period 1659 to 1995. Earth and Planetary Science Letters 228, 177–194 http://dx.doi.org/10.1016/j.epsl.2004.09.028.